

Review

# Carbon Nanostructures for Tagging in Electrochemical Biosensing: A Review

Paloma Yáñez-Sedeño \*, Susana Campuzano and José M. Pingarrón

Departamento de Química Analítica, Facultad de CC. Químicas, Universidad Complutense de Madrid, E-28040 Madrid, Spain; susanacr@quim.ucm.es (S.C.); pingarro@quim.ucm.es (J.M.P.)

\* Correspondence: yseo@quim.ucm.es; Tel.: +34-91-394-4315; Fax: 34-91-394-4329

Academic Editor: Jandro L. Abot

Received: 28 November 2016; Accepted: 11 January 2017; Published: 16 January 2017

**Abstract:** Growing demand for developing ultrasensitive electrochemical bioassays has led to the design of numerous signal amplification strategies. In this context, carbon-based nanomaterials have been demonstrated to be excellent tags for greatly amplifying the transduction of recognition events and simplifying the protocols used in electrochemical biosensing. This relevant role is due to the carbon-nanomaterials' large surface area, excellent biological compatibility and ease functionalization and, in some cases, intrinsic electrochemistry. These carbon-based nanomaterials involve well-known carbon nanotubes (CNTs) and graphene as well as the more recent use of other carbon nanoforms. This paper briefly discusses the advantages of using carbon nanostructures and their hybrid nanocomposites for amplification through tagging in electrochemical biosensing platforms and provides an updated overview of some selected examples making use of labels involving carbon nanomaterials, acting both as carriers for signal elements and as electrochemical tracers, applied to the electrochemical biosensing of relevant (bio)markers.

**Keywords:** electrochemical biosensing; carbon nanostructures; advanced labels; amplification

## 1. Introduction

Nowadays, there is a huge demand for fast, reliable and low-cost analytical systems for the detection and quantification of biomolecules of relevance in different fields. In this context, electrochemical biosensing is considered as a particularly well suited strategy for this purpose due to its inherent high sensitivity, simplicity of the operational procedure, easy availability and affordable cost of the required equipment together with possibility of miniaturization and suitability for in-field applications.

Interestingly, biosensing using electroanalytical techniques is playing a more and more important role in DNA and protein analysis. Moreover, the growing research in advanced nanomaterials has significantly impacted this field by providing a great variety of novel, versatile and rationally designed nanostructured supports for transduction, signal generation and amplification in biosensing. In parallel with these major advances in nanotechnology, the wide variety of bioreceptors explored and the versatility of design and modification offered by electrochemical substrates have also played major roles in the outstanding capabilities demonstrated by electrochemical biosensors.

Carbon nanomaterials can offer various signal amplification routes in electrochemical biosensing implying their use as electrode materials, carriers for signaling elements, separators and collectors, catalysts, mediators to regulate the electron transfer process or a combination of some of these characteristics [1]. Their large surface area, excellent biological compatibility and ease and well-documented organic functionalization make carbon-based nanomaterials excellent carriers for loading numerous signal elements such as enzymes, oligonucleotides, antibodies, redox molecules and inorganic nanomaterials to greatly amplify the transduction signals of recognition events in electrochemical

bioassays [1–3]. Apart from commonly used 1D and 2D carbon nanomaterials, other 3D carbon nanostructures such as mesoporous carbon nanospheres [4–6] have been demonstrated to be good candidates as carriers for loading signaling molecules such as enzymes, antibodies and AuNPs for developing very sensitive immunosensors. Carbon nanospheres possess better tenability and homogeneity of particle size compared to CNTs, and porous nanostructure for large loading of guest molecules. Moreover, their “green” and cost-effective synthesis under hydrothermal conditions means they can be produced homogeneously and with surface-functional groups and good biocompatibility [5]. In the following sections, we provide an updated overview of the latest applications of several carbon nanomaterials and their hybrid nanocomposites, as both carriers for signal elements and tracers based on their direct electrochemistry, in the development of novel DNA biosensors and immunosensors. Classification is made according to both the type of bioreceptor and the employed carbon nanomaterial with the aim of conducting a critical evaluation of their characteristics and performance.

## 2. Carbon Nanomaterials Used as Carriers for Signal Elements in Electrochemical DNA or Aptamer-Based Sensors

Electrochemical DNA sensing has gained considerable interest because of inherent high sensitivity, rapid response, low cost and simplicity of miniaturization. Combining signal amplified DNA sensing and electrochemical transduction provides a new avenue to develop ultrasensitive nucleic acid detection technology widely demanded nowadays for routine analysis, *point-of-care* (POC) and portable device applications [7,8]. Because of their large surface area, excellent biological compatibility and easy functionalization, carbon-based nanomaterials such as carbon nanotubes (CNTs) and graphene have been widely used as excellent carriers for loading numerous signal elements such as enzymes [9], mimic enzymes [10,11], oligonucleotides [12,13] redox reporters [14,15] or combination [7,8]. These elements can greatly amplify the transduction signals of recognition events and simplify the protocols used in electrochemical DNA assays [1,15]. The selected approaches, discussed briefly below, will clearly illustrate the different electroactive elements and connection modes between signal elements and carbon nanomaterials reported so far.

CNTs are inherently lightweight and exhibit, apart from unique electronic, chemical, and mechanical properties, high surface area to volume ratio coupled with large aspect ratios and abundant surface sites for functionalization. Both single- and multi-walled carbon nanotubes (SWCNTs and MWCNTs, respectively) have been used as carriers for loading large amounts of redox mediator molecules [7] or enzyme tags [9] to amplify the electrochemical signals in DNA biosensing. Most of these attempts have focused on enzyme tracers due to the multiple enzymatic turnovers achieved at these bioconjugates which significantly amplify the electrochemical response [8,9]. Unlike functionalization of dendrimers which requires sequential steps to achieve a high degree of labeling, a large number of labels can be easily loaded on an individual nanotube in a single-step conjugation reaction (i.e., a monolayer of 500 to 9600 molecules conjugated on a CNT 0.8–2.0  $\mu\text{m}$  average length) [8]. Moreover, these externally conjugated labels on CNT platforms are capable of generating measurable signals without requiring releasing steps as other carriers based on encapsulation techniques [8].

Wang et al. [16] reported in 2004 an ultrasensitive electrochemical DNA biosensor involving the use of streptavidin-functionalized magnetic beads (Strept-MBs) and a dual amplification route combining the use of a CNT-amplifying label (9600 alkaline phosphatase (ALP) molecules per SWCNT) and a CNT-modified electrode for pre-concentration of the ALP-catalyzed enzymatic product generated in the presence of 1-naphthyl phosphate. Using chronoamperometry, the method allowed the detection of synthetic DNA down to  $54 \text{ amol} \cdot \text{L}^{-1}$ . Further sensitivity enhancement ( $5.4 \text{ amol} \cdot \text{L}^{-1}$ ) was reported one year later by the same research group [17] using an electrostatic layer-by-layer (LBL) self-assembly of 4-layer ALP films (total 196,000 molecules) on an individual SWCNT (3  $\mu\text{m}$  average length). Gao et al. [9] described a method for ultrasensitive DNA sensing using a molecular beacon as a selective capture probe and streptavidin–horseradish peroxidase (HRP) functionalized CNTs to amplify

the electrochemical signal. This bio-scaffold was prepared by immobilizing the molecular beacon labeled with biotin and thiol at 5' and 3' ends on a glassy carbon electrode (GCE) modified with gold nanoparticles (AuNPs) and 1-pyrenebutyrate functionalized graphene (PFG) (Figure 1). In the absence of target DNA, the molecular beacon is in the closest state and the biotin label is sterically shielded and, therefore, inaccessible to the reporter enzyme. However, after hybridization with the target DNA, the biotin end of the molecular beacon MB was forced away from the electrode allowing the binding of streptavidin-HRP labelled CNTs which catalyzed the oxidation of *o*-phenylenediamine (*o*-PD) and  $\text{H}_2\text{O}_2$  leading to a significantly amplified differential pulse voltammetric signal. The biosensor response was logarithmically related to the target concentration from  $10 \text{ amol}\cdot\text{L}^{-1}$  to  $1 \text{ pmol}\cdot\text{L}^{-1}$ , the LOD was  $2.8 \text{ amol}\cdot\text{L}^{-1}$ , and an excellent selectivity to differentiate single-base mismatched and three-base mismatched sequences of DNA was achieved.

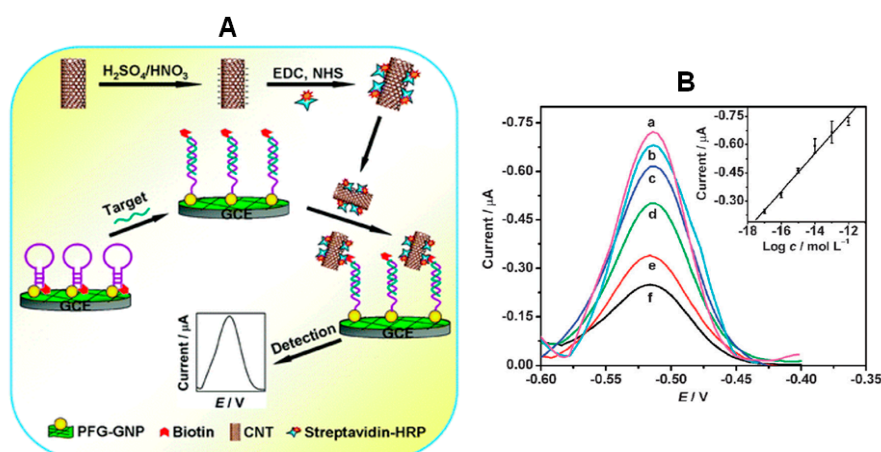


**Figure 1.** (A) Schematic display of the DNA electrochemical detection approach developed using a molecular beacon immobilized onto a glassy carbon electrode (GCE) modified with gold nanoparticles (AuNPs) and 1-pyrenebutyrate functionalized graphene (PFG), and streptavidin–horseradish peroxidase (HRP)–carbon nanotubes (CNTs). EDC: 1-(3-(dimethylamino)-propyl)-3-ethylcarbodiimide hydrochloride; NHS: N-hydroxysulfosuccinimide. See the text for more information; (B) differential pulse voltammetry (DPV) curves obtained at different target concentrations: 1 pM (a), 100 fM (b), 10 fM (c), 1 fM (d), 100 aM (e) and 10 aM (f). Inset: linear relationship between peak current and the logarithm of target DNA concentration. Reprinted and adapted from [9] with permission.

A sensitive and label-free electrochemical method involving DNA phosphorylation analysis was developed for determination of T4 polynucleotide kinase (PNK) activity and inhibition by using DNA wrapped aminoferrocene (Fc)-SWCNTs (DNA/Fc-SWCNTs) and  $\text{Ti}^{4+}$  [7]. In this method, a thiolated DNA containing 5'-hydroxyl group was self-assembled onto a gold electrode and used as substrate for PNK. The biofunctionalized SWCNTs with anchored DNA and Fc was chosen as the signal indicator by virtue of the intrinsic 5'-phosphate end of anchored DNA and the high loading of Fc for electrochemical signal generation and amplification. The 5'-hydroxyl group of the substrate DNA on the electrode was phosphorylated by T4 PNK in the presence of ATP, and the resulting 5'-phosphoryl end product could be linked with  $\text{Ti}^{4+}$ , which selectively binds phosphorylated DNA over non-phosphorylated DNA. When exposing the  $\text{Ti}^{4+}$ -DNA modified electrode to DNA/Fc-SWCNT bioconjugates, the latter were linked through the interaction between  $\text{Ti}^{4+}$  and phosphate groups in the substrate DNA and anchored DNA (Figure 2). Owing to the linkage, the Fc modified on the SWCNTs was positioned in close proximity to the electrode and the facile electron-transfer reaction between Fc and the electrode surface, measured by DPV, was proportional to the activity of T4 PNK. This assay can measure T4 PNK activity down to  $0.01 \text{ U}\cdot\text{mL}^{-1}$ . The developed method exhibits potential utility in research of interactions between proteins and nucleic acids and provides a diversified platform for a kinase activity assay.

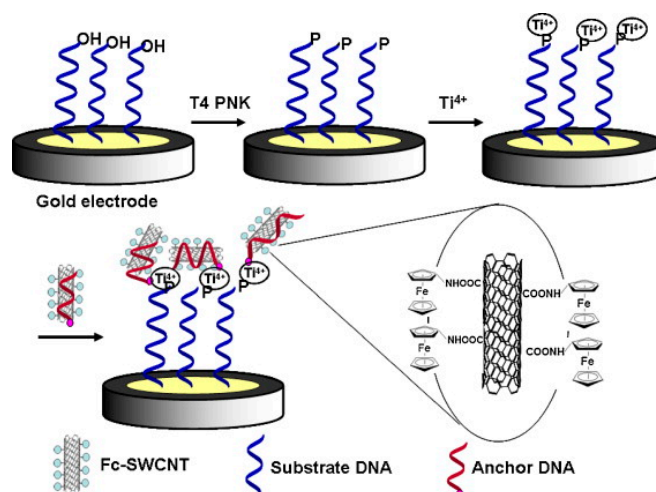


**Figure 2.** Schematic illustration of the electrochemical assay for the detection of kinase activity using DNA/Fc-single-walled carbon nanotubes (DNA/Fc-SWCNTs) and  $\text{Ti}^{4+}$ . See the text for more information. Reprinted from [7] with permission.

An ultrasensitive electrochemical sandwich hybridization assay for the detection of human acute lymphocytic leukemia (ALL)-related *p185 BCR-ABL* fusion transcript was reported by using CNTs as HRP carriers [8]. The carboxylated CNTs, dual functionalized with HRP molecules and target-specific 18 bp detection probes via diimide-activated amidation were used to label and amplify the target hybridization signal. In this approach, the target DNA was sandwiched between the amino terminated capture probe covalently immobilized onto HOOC-magnetic beads (MBs) and detection probes immobilized on the CNTs (Figure 3). The electroactive enzymatic product, formed by incubation of the final modified MBs with 2-aminophenol- $\text{H}_2\text{O}_2$  was measured by square wave voltammetry (SWV) at a screen-printed carbon electrode (SPCE). The assay allowed an LOD of  $83 \text{ fmol} \cdot \text{L}^{-1}$  and a 4-order-wide dynamic range for the determination of synthetic short (46 bp) target. The resulting assay also allowed a robust discrimination between the perfect match and a three-base mismatch sequence and a LOD of  $1 \times 10^{-16} \text{ mol}$  in  $60 \mu\text{L}$  full-length (491 bp) DNA oncogene, which enabled the PCR-free detection of target transcripts using only 65 ng of mRNA extracted from the *p185 BCR-ABL*-positive human leukemic SUP-B15 cell line.

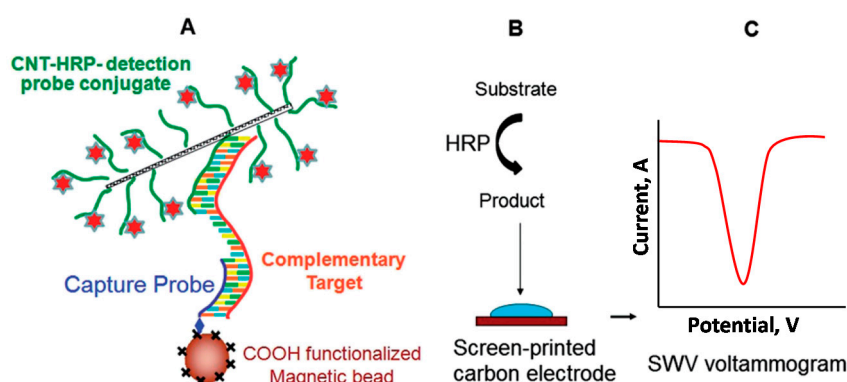


**Figure 3.** Schematic display of the electrochemical approach developed using a sandwich hybridization assay performed onto functionalized magnetic microbeads (HOOC-MBs) and HRP-tagged CNTs as labels. (A) Sandwich hybridization assay performed on MBs; (B) targets quantification by measuring the electroactive enzymatic product; (C) The resulting square-wave voltammetry (SWV) voltammogram showing a well-defined reduction peak for TG/*p185*-ssDNA/mRNA targets. Reprinted from [8] with permission.



In contrast to graphene, graphene oxide is electroactive and can undergo electrochemical reduction [13]. Furthermore, GO with large negatively charged functional groups can also serve as a carrier for positively charged species through strong electrostatic interactions [1]. Two simple label-free electrochemical aptasensors for thrombin and ATP have been reported, making use of methylene blue-anchored GO as signal amplification nano-platforms and taking advantage of the specific binding affinity of the aptamer towards the target and the different affinities of GO for methylene blue, ssDNA, dsDNA, and G-quadruplex [14]. In this approach, specific aptamers were designed to both specifically recognize the analyte-binding and also bind GO onto the electrode. A thiolated modified thrombin binding aptamer (TBA) was self-assembled on a gold electrode to determine thrombin, while for the ATP sensor, the ATP-binding aptamer (ABA) was immobilized via the partial hybridization reaction between ABA and the anchored DNA previously assembled on the gold electrode. After aptamer immobilization on the electrode, GO was readily fixed on the electrode through the free DNA bases and abundant methylene blue molecules were anchored to the GO by electrostatic interaction, leading to a strong differential pulse voltammetry (DPV) signal in the absence of target. When thrombin is present, the formation of an aptamer-thrombin G-quadruplex structure avoids  $\pi$ - $\pi$  stacking interaction between TBA and GO and, consequently, draws GO together with plenty of methylene blue far away from the electrode surface thus resulting in a sharply decreased DPV signal. However, in the presence of ATP, the ABA switches its structure to bind ATP and prefers to form an ATP-aptamer complex rather than an aptamer-DNA duplex. As a result, only five base pairs are left to hybridize with anchored DNA, which is unstable at room temperature and results in the dissociation of ABA. The release of ABA is accompanied by the extrication of abundant GO and methylene blue anchored by GO, which offers a significant amplification in the capture event. By monitoring the change of the reduction peak current of methylene blue ( $i_p$ ) before and after analyte binding, selective and sensitive target detection could be realized.

Li et al. [15] reported an electrochemical method for gene-specific methylation detection and methyltransferase (MTase) activity/inhibition assay using *HpaII* endonuclease and redox reported tagged GO to improve the selectivity and sensitivity of the assay, respectively. Methylation in higher eukaryotic cells has frequently been observed at carbon 5 position of cytosine (C) in the 5'-CG-3' sequence (CpG). A specific thiolated DNA was assembled on AuNPs-modified GCE. The reporter (thionine), was conjugated at the 3'-end of the immobilized capture DNA probe via GO. After hybridization with the target DNA (one 137 mer DNA from exon 8 promoter region of the human *p53* gene, was extracted from HCT116 cells), methylation of the DNA hybrid (under catalysis of M.SssI MTase) and cleaved by *HpaII* endonuclease, electrochemical signals of the reporter, measured by DPV, decreased. Since the cleavage of the endonuclease is blocked by CpG methylation, the voltammetric signal after cleavage is related to the methylation status and MTase activity, which forms the basis of this approach for MTase activity assay and site-specific methylation determination. The electrochemical signal provided a linear relationship with M.SssI activities ranging from 0.1 to 450 U·mL<sup>-1</sup> with a LOD of  $\sim(0.05 \pm 0.02)$  U·mL<sup>-1</sup> (S/N = 3).

GO nanoplatelets (GONPs) are much smaller than the traditional graphene sheets and with higher uniformity of the sizes. They possess an extraordinary electrochemistry able to lead to a high amplification of the electrochemical signal. Indeed, GONPs have demonstrated to be outstanding voltammetric labels in biosensing in a similar manner to metallic nanoparticles, due their inherent reduction signal [12,13]. Moreover, the use of GONPs labels over metal nanoparticles has the strong advantage of not involving the use of any corrosive or toxic chemicals [13]. Bonnani et al. [12] proposed for the first time the use of GONPs as electroactive labels for the discrimination of single-nucleotide polymorphism correlated with Alzheimer's disease. These authors explored the different ability of GONPs to conjugate to DNA hybrids obtained with complementary, non-complementary and one-mismatch sequences by physical adsorption of the corresponding probe onto GONPs-modified disposable electrochemical-printed carbon electrodes (DEP-chip). The working signal, coming from the reduction of the oxygen-containing groups present on the surface of GONPs, was measured by

DPV at the DEP-chip. GONPs were also used as inherently electroactive labels for thrombin (THR) aptasensing [13]. The basis of detection lies in the ability of GO to be electrochemically reduced, thereby providing a well-defined reduction wave; one GONP of dimension  $50 \times 50$  nm can provide a reduction signal by accepting  $\sim 22,000$  electrons. In this approach, a specific thrombin aptamer (APT-15) was immobilized onto the surface of a disposable electrical printed (DEP) electrode by dry physical adsorption. In the presence of thrombin, the aptamer bound specifically to the protein and is partially removed from the electrode surface due to conformational changes. GONPs are then adsorbed onto the remaining immobilized THR-APT-15 due to the strong  $\pi$ - $\pi$  interactions. In the absence of thrombin, more GONPs were adsorbed due to the high loading of THR-APT-15 immobilized on the electrode (Figure 4). This label-free aptasensing approach allowed the selective determination of thrombin in the  $3 \text{ pmol} \cdot \text{L}^{-1}$ – $0.3 \text{ mmol} \cdot \text{L}^{-1}$  concentration range.

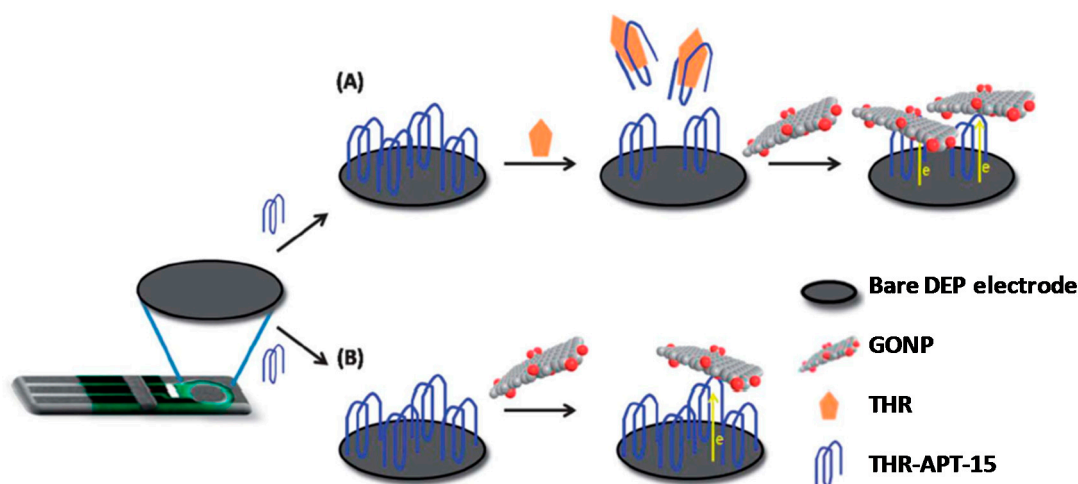


**Figure 4.** Illustration of the utilization of GO nanoplatelets (GONPs) in label-free electrochemical aptasensing of thrombin. See the text for more information. Reprinted and adapted from [13] with permission.

HRP has been extensively used in many fields due to its excellent catalytic activity [18]. Indeed, loading HRP on various nanomaterials has become a common and useful way to further amplify the detection signals and achieve lower detection limits. However, the relative large size of HRP limits its maximum loading amount, which is adverse to signal amplification. Furthermore, as a natural enzyme, its activity is highly dependent on protein conformation, leading to the vulnerability to external conditions. Thus, HRP mimicking is of great importance and remains a challenging topic [5]. Since the catalytic center of HRP is actually an iron-containing porphyrin complex, mimicking the biological function of HRP using iron porphyrin such as hemin [10,19] and iron(III) meso-tetrakis(*N*-methylpyridinium-4-yl)porphyrin (FeTMPyP) [11] has attracted considerable interest. However, free ferric porphyrins usually show much weaker peroxidase activity than HRP in aqueous solution, which can be attributed to the oxidative destruction and the self-aggregation of ferric porphyrin molecules to form catalytically inactive species [5]. Therefore, in order to achieve good catalytic performance, the key point in the design of HRP mimicking analogues is to choose a suitable carrier for loading the ferric porphyrin molecules while maintaining their intrinsic peroxidase activity. In this sense, apart from G-quadruplex DNA oligomers [10,20], GO has also been demonstrated to be a successful carrier for hemin [19] as well as carboxylic GO for hemin [10] and FeTMPyP [11] endowing these iron porphyrins with high peroxidase activity [10]. Compared with graphene–hemin complex, the carboxylic graphene–hemin complex not only possesses high catalytic activity, but also exhibits excellent water dispersibility [11].

A pseudobienzyme-channeling amplified electrochemical aptasensor for thrombin was developed by coupling 3,4,9,10-perylenetetracarboxylic acid (PTCA)/hemin nanocomposites as redox probes and electrocatalysts with glucose oxidase (GOx) immobilized on the aptasensor surface [19]. The PTCA/hemin nanocomposite was casted on a gold disk electrode and, after AuNPs deposition, the thiol-terminated thrombin aptamer (THRA) self-assembled onto the surface of the AuNPs/PTCA/hemin/Au electrode. A droplet of GO-labeled complementary thrombin aptamer (GO-CTBA) was placed on the modified electrode to obtain a GO-CTBA/THRA/AuNPs/PTCA/hemin/Au electrode by hybridization between THRA and CTHRA. The resulting electrode was incubated in a GOx solution. In this approach, GOx serves as a blocking reagent to block possible remaining active sites and avoid nonspecific adsorption and, by bioelectrocatalyzed reduction of glucose, produces  $\text{H}_2\text{O}_2$ , which in turn was electrocatalyzed by the PTCA/hemin nanocomposites. These catalytically linked enzymatic reactions lead to signal amplification and therefore increase the biosensor sensitivity. The incubation with thrombin led to the release of GO-CTHRA from the self-assembled duplex on the electrode into solution, thus decreasing the steric hindrance of the aptasensor and enhancing the electrochemical signal (CV monitoring of the reduction signal of the PTCA/hemin in the presence of glucose). This approach allowed a linear relationship for thrombin determination from  $0.005$  to  $20 \text{ nmol}\cdot\text{L}^{-1}$  and a LOD of  $0.001 \text{ nmol}\cdot\text{L}^{-1}$  and feasibility to perform the determination of the target protein in spiked human blood serum.

Wang et al. [10] designed a new DNA biosensing approach by combining the use of a biotinylated molecular beacon with a novel peroxidase mimic, prepared by loading ferric porphyrin (FeTMPyP) and streptavidin onto carboxylic GO as trace label to recognize the biotinylated beacon (Figure 5). A gold nanoparticles-single-walled carbon nanohorn (AuNPs-SWCNH) composite-modified glassy carbon electrode was used to immobilize the biotinylated molecular beacon, and the mimic was prepared by assembling FeTMPyP on both sides of GO via  $\pi$ - $\pi$  stacking and labeling with streptavidin by an amidation reaction. In the absence of target DNA, the molecular beacon probe was in the “closed” state, and the interaction with the streptavidin on the trace label was blocked due to the large steric effect. Conversely, after hybridization with target DNA, the resulting rigid duplex structure of the beacon probe moved the biotin group away from the electrode surface, making the biotin end easily accessible to the trace label. The hybridization event was followed by DPV monitoring of the o-phenylenediamine (o-PD) oxidation in the presence of  $\text{H}_2\text{O}_2$ . This “signal on” electrochemical biosensor using a graphene-supported ferric porphyrin as a HRP mimicking trace label allowed a linear relationship with the target concentration over 5 orders of magnitude ( $10 \text{ pmol}\cdot\text{L}^{-1}$ – $100 \text{ amol}\cdot\text{L}^{-1}$ ) and a LOD of  $22 \text{ amol}\cdot\text{L}^{-1}$  (at  $3\sigma$ ). This LOD was much lower than that obtained with a HRP-based trace label thus demonstrating the greatly enhanced peroxidase activity of the porphyrin-based HRP mimic.

A simple, sensitive, and label-free method for microRNAs biosensing based on a sandwich hybridization assay using a hairpin DNA capture probe, bio bar code functionalized AuNPs and carboxylic graphene-hemin hybrid nanosheets as mimic enzyme catalysis signal amplification was reported [11]. In this method, a thiolated hairpin probe was assembled onto AuNPs-GCE, the target miRNA was sandwiched between the hairpin probe, and the bio bar code functionalized AuNPs, and finally incubated with carboxylic graphene-hemin complex (activated by EDC/NHS) for covalent immobilization onto the  $-\text{NH}_2$  groups at the 3'-end of one of the two types of DNA probes assembled on the bio bar code. Results demonstrated that the AuNPs functionalized biobarcodes allowed the capture of more carboxylic graphene-hemin complex. The intrinsic peroxidase-like activity of hemin on the carboxylic graphene surface was used to catalyze the oxidation reaction of hydroquinone (HQ) in the presence of  $\text{H}_2\text{O}_2$ . The electrochemical reduction current of the oxidative product of benzoquinone, dependent on the hybridization amount of microRNAs, was monitored by DPV. Using this graphene-hemin-based approach, the current response was proportional to the logarithm concentration of microRNA-159a from  $0.5 \text{ pmol}\cdot\text{L}^{-1}$  to  $1.0 \text{ nmol}\cdot\text{L}^{-1}$  with a LOD of  $0.17 \text{ pmol}\cdot\text{L}^{-1}$  ( $S/N = 3$ ).

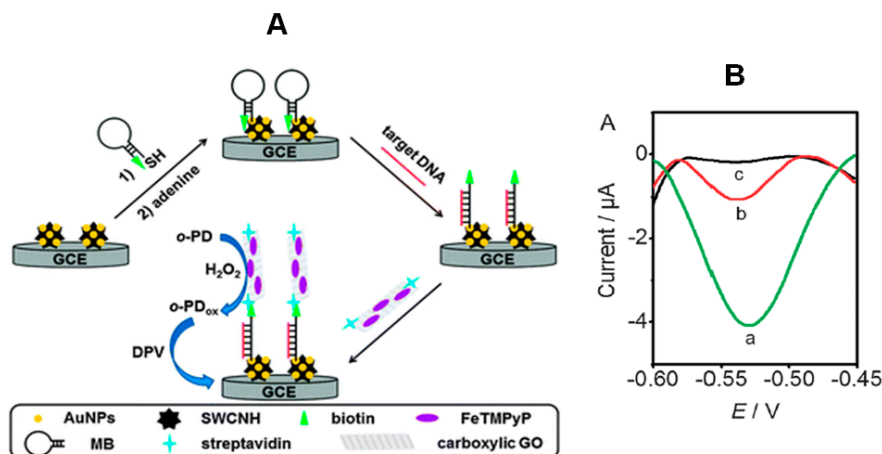


**Figure 5.** (A) Schematic illustration of the electrochemical DNA biosensing approach based on the use of a molecular beacon (MB) and a graphene-supported ferric porphyrin as a peroxidase mimic; (B) DPV responses obtained with (a) FeTMPyP–streptavidin–GO and (b) HRP–streptavidin–GO as trace label and (c) without trace label at 10 fM target DNA. See text for more information. Reprinted and adapted from [10] with permission.

### 3. Carbon Nanomaterials Used as Carriers for Signal Elements in Electrochemical Immunosensors

Carbon nanomaterials have been also widely used in the design of electrochemical immunosensors. Electrode nanostructuring with CNTs or graphene and their hybrids is currently a regular operation for preparing electrochemical scaffolds with improved conductivity and enhanced ability for biomolecules immobilization. In addition, other types of carbon nanoforms such as carbon nanohorns, graphene quantum dots, fullerene (C<sub>60</sub>) or carbon nanoparticles have emerged recently that also demonstrate the ability to improve the analytical performance of these devices. Along with the use of carbon nanomaterials for the construction of nanostructured electrode surfaces, their utilization as carriers of elements for electrochemical signal amplification is another less widespread but equally relevant application.

The importance of the use of nanomaterials as signal tags for amplification of electrochemical responses is reflected in the number of reviews published on this topic. Pei et al. [21] reviewed sandwich-type immunosensors and immunoassays exploiting nanostructured labels; Lei and Ju [22] discussed the applications of functional nanomaterials as signal amplification tools for biosensing, and Ding et al. [23] illustrated the use of nanoparticle labels, including carbon nanomaterials, for signal amplification in electrochemical affinity biosensors. More recently, the applications of nanomaterials as versatile tools for signal amplification in (bio)analysis [24], and specifically with electrochemical immunosensors [25] were also reviewed.

As it is well known, electrochemical immunosensors are characterized by excellent analytical capabilities such as high sensitivity, selectivity, reproducibility, simplicity of construction and use, and feasible miniaturization. These important advantages become more evident insofar as the immunoreagent attachment and the transduction event are more efficient. Once an electrode platform with good capacities for biomolecules immobilization has been prepared, the detection of electrochemical signals associated to the antigen-antibody interaction requires the use of appropriate labels. Enzymes such as ALP or HRP, or electroactive materials such as thionine or Fc, have been usually employed for this purpose [21]. However, in these conventional designs, the low number of labels participating in each immunocomplexation event results in low sensitivity. Nanomaterials can increase the loading of electrochemically detectable species as well to catalyze the electrolysis of a large quantity of substrate, which enhances the electrochemical signal [23]. Hence, the possibility of using



nanomaterials as labels has been exploited in the development of electrochemical immunosensors, this leading to new perspectives in this field.

This section focuses on recent examples exploiting carbon nanomaterials as signal tags in the design of electrochemical immunosensors. As it is shown, current enhancement associated with this strategy, often combined with the use of nanostructured electrode surfaces to measure larger intensities, provides the basis for sensitive detection of disease-related biomarkers in biological samples, as well as other important compounds present at trace levels in clinical, food and environmental samples. Moreover, due to the high number of recently published papers making use of this detection strategy, this section has been divided into three parts corresponding to the use of carbon nanotubes, graphene and other carbon nanomaterials. In addition, for better understanding, the most relevant examples within each of these subsections have been summarized in the form of tables showing the fundamentals and analytical characteristics of each configuration.

### 3.1. Carbon Nanotubes Used as Carriers for Signal Elements in Electrochemical Immunosensors

Table 1 allows us to conclude that most of the designs of electrochemical immunosensors using CNTs as label tags for signal amplification are sandwich-type configurations where the capture antibody is immobilized onto an electrode scaffold prepared with highly conductive and good bonding materials, and the detection antibody is linked to the amplification label. In general, the detection step relies on the measurement of current from  $\text{H}_2\text{O}_2$  and, therefore, the electrochemical tags used as labels contain one or more elements (e.g., metallic NPs, oxide NPs, or redox mediators) showing electrocatalytic activity toward such an electrochemical process. This is a common strategy in the development of electrochemical immunosensors for the determination of cancer biomarkers where, besides the inherent selectivity of antibody-antigen reactions, a high sensitivity is required in many cases which can be improved by the use of labels increasing the number of active sites and the magnitude of current related with specific interactions. A representative example of this strategy is the preparation of an electrochemical immunosensor for interleukin 6 (IL-6), a biomarker overexpressed in head and neck squamous cell carcinomas (HNSCC). The determination of this cytokine at the required low levels could be performed by using a sensitive electrochemical immunosensor prepared by immobilization of the capture antibody onto a forest-SWCNTs-modified GCE and the secondary antibodies attached to a multi-peroxidase label consisted of carboxylated MWCNTs containing 106 HRP labels per 100 nm. The analytical utility of the developed immunosensor was demonstrated by determining the IL-6 secreted from a panel of HNSCC cells obtaining results well correlated with those provided by the standard ELISA assay [26]. Epstein-Barr virus (EBV) is frequently found in Burkitt's or Hodgkin's lymphomas and nasopharyngeal carcinoma. EBV-derived latent membrane protein 1 (LMP-1) is essential for B-lymphocyte growth transformation [27] and thus, the detection of low levels of LMP-1 biomarker has a great interest. In a recent paper, a GCE modified with graphene sheets and MWCNTs, and a nanolabel prepared with a composite of carbon nanotubes and Pd@Pt nanoparticles, were proposed for the preparation of a sandwich-type electrochemical immunosensor for LMP-1 (Figure 6). Pd@Pt nanoparticles were synthesized according to the solution-phase synthesis method. Briefly, Pluronic F127 was ultrasonically dissolved in an aqueous solution containing  $\text{K}_2\text{PtCl}_4$  and  $\text{Na}_2\text{PdCl}_4$  in 6 M hydrochloric acid medium. After adding ascorbic acid (AA) as a reducing agent, the mixture was continuously sonicated in a water bath for 4 h at 35 °C. The final product was collected and washed with acetone and water in consecutive washing/centrifugation cycles for five times and then dried at room temperature. An amplified DPV signal was obtained taking advantage of the synergistic effect between metallic nanoparticles and HRP in the presence of  $\text{H}_2\text{O}_2$  and thionine (Thi) [28].

An electrochemical nanostructured immunosensor for the breast cancer biomarker carbohydrate antigen 15-3 (CA15-3) was fabricated using MWCNTs-supported numerous ferritin as labels for the detection antibody taking advantage of the enzyme-mimic activity of this protein. Furthermore, additional current amplification was attained by immobilization of capture antibodies onto graphene

oxide functionalized with 1-pyrenecarboxylic acid (Py-COOH). It should be noted that this non-covalent functionalization was established by irreversible adsorption on the GO surface where the pyrenyl strongly interacts through  $\pi$ -stacking. The detection of CA15-3 was based on the enhanced bioelectrocatalytic reduction of  $\text{H}_2\text{O}_2$  in the presence of a high number of ferritins mediated by HQ at the GO/Py-COOH-modified electrode [29]. As Table 1 shows, a wide linear range from 0.05 to  $100 \text{ U}\cdot\text{mL}^{-1}$  CA15-3 was obtained, and the developed immunosensor was applied to the analysis of serum with good results.

Various designs of electrochemical immunosensors for the detection of carcinoembryonic antigen (CEA) involved the use of CNTs as signal labels. For example, a composite prepared by assembling HRP and the secondary antibodies onto AuNPs-polyaniline (PANI)-functionalized MWCNTs was prepared and used as carrier tags for the immunosensing determination of the protein. A high content of HRP on the surface of AuNPs-PANI@CNTs contributes to amplifying the electrochemical responses in a sandwich assay configuration where the capture anti-CEA antibody was immobilized onto an AuNPs/thionine/MWCNTs/GCE [30]. The same group also prepared an electrochemical immunosensor for the simultaneous determination of CEA and  $\alpha$ -fetoprotein (AFP) by means of an original design involving two different metal ion labels,  $\text{Pb}^{2+}$  and  $\text{Cd}^{2+}$ , for the respective signals amplification. AuNPs@MWCNTs were used as carriers to immobilize secondary antibodies and distinguishable lead or cadmium ions electrochemical tags. The reduction responses from metal ions at AuNPs/AuE using square-wave voltammetry (SWV) were proportional to the protein biomarkers concentration over the useful ranges and, interestingly, the high content of metal ion labels on the carrier could be voltammetrically detected without need of acid dissolution, thereby providing a high response amplification [31]. As Table 1 shows, the detection strategy used provided a great sensitivity with LOD values of  $3.0$  and  $4.5 \text{ pg}\cdot\text{mL}^{-1}$  for CEA and AFP, respectively [31]. Another immunosensor configuration for the simultaneous determination of CEA and AFP was developed by Lai et al. [32]. Streptavidin-functionalized silver-nanoparticle-enriched MWCNTs were designed as trace tags for multiplexed measurements using a disposable immunosensor array. The AgNPs/MWCNTs were functionalized with streptavidin for further immobilization of biotinylated signal antibodies. A sandwich immunoassay was performed with capture antibodies immobilized onto chitosan-modified SPCEs in such a way that a high number of AgNPs were captured onto every single immunocomplex and further amplified by deposition of silver to obtain an electrochemical stripping response. The developed method resulted in a highly sensitive proposal for application in clinical samples due to the electrochemical-stripping signal of the AgNPs that allowed us to obtain detection limits down to  $0.093$  and  $0.061 \text{ pg}\cdot\text{mL}^{-1}$  for CEA and AFP, respectively. Furthermore, the assay results of serum samples with the proposed method were in acceptable agreement with the reference values. Yang et al. [33] prepared an amperometric immunosensor for CEA involving MWCNTs decorated with concanavalin A (Con A) and HRP-labeled secondary antibodies. Con A possesses multiple sites with high affinity for sugar chains located on HRP, and this leads to more  $\text{Ab}_2$ -HRP immobilized on the probe surface. Therefore, a high sensitivity was attained by performing a sandwich-type configuration with the capture antibody covalently immobilized onto a gold electrode modified with cysteine.

**Table 1.** Electrochemical immunosensors using CNTs as labels.

Electrode	Label	Analyte	Immunoassay	Technique	Linear Range	LOD	Sample	Reference
fSWCNTs/PG	HRP-MWCNTs	IL-6	Sandwich with immobilized anti-IL-6 and Ab <sub>2</sub> -label. H <sub>2</sub> O <sub>2</sub> + HQ as the redox probe	amperom.	0.5–30 pg·mL <sup>−1</sup>	0.5 pg·mL <sup>−1</sup>	HNSCC cells	[26]
graphene/MWCNTs/Chit/GCE	HRP/Pd@Pt/MWCNTs	LMP-1	Sandwich with immobilized anti-LMP-1 and Ab <sub>2</sub> -label. H <sub>2</sub> O <sub>2</sub> /THI as the redox probe	DPV	0.01–40 ng·mL <sup>−1</sup>	0.62 pg·mL <sup>−1</sup>	spiked serum	[28]
HOOC-Py/GO/Cys-AuE	MWCNTs/ferritin	CA15-3	Sandwich with immobilized anti-CA15-3 and Ab <sub>2</sub> -label. H <sub>2</sub> O <sub>2</sub> + HQ as the redox probe	DPV	0.05–100 U·mL <sup>−1</sup>	9 ± 0.6 mU·mL <sup>−1</sup>	serum	[29]
AuNPs/THI-MWCNTs/GCE	HRP/AuNPs/PANI@MWCNTs	CEA	Sandwich with immobilized anti-CEA and Ab <sub>2</sub> -label. H <sub>2</sub> O <sub>2</sub> as the redox probe	DPV	0.02–80.0 ng·mL <sup>−1</sup>	8.0 pg·mL <sup>−1</sup>	serum	[30]
AuNPs/AuE	AuNPs@MWCNTs-Pb <sup>2+</sup>	CEA	Multiplex sandwich with immobilized anti-CEA or anti-AFP. Pb <sup>2+</sup> or Cd <sup>2+</sup> as the redox probes	SWV	0.01–60 ng·mL <sup>−1</sup>	3.0 pg·mL <sup>−1</sup>	serum	[31]
	AuNPs@MWCNTs-Cd <sup>2+</sup>	AFP				4.5 pg·mL <sup>−1</sup>		
Chit/SPCE	Strept-AgNPs/MWCNTs	CEA	Multiplex sandwich with immob. anti-CEA or anti-AFP. Biotin-Ab <sub>2</sub> -label. Ag as the redox probe.	LSSV	0.0001–5.0 ng·mL <sup>−1</sup>	0.093; 0.061 pg·mL <sup>−1</sup>	serum	[32]
		AFP						
L-Cys-AuE	HRP/ConA/HRP/PDDA/MWCNTs	CEA	Sandwich with immobilized anti-CEA and Ab <sub>2</sub> -label. H <sub>2</sub> O <sub>2</sub> + HQ as the redox probe	DPV	0.05–5 ng·mL <sup>−1</sup> 5–200 ng·mL <sup>−1</sup>	0.018 ng·mL <sup>−1</sup>	serum	[33]
APTES/graphene/GCE	MWCNTs-NH <sub>2</sub> /PdPt NCs	CEA	Sandwich with immobilized anti-CEA and Ab <sub>2</sub> -label. H <sub>2</sub> O <sub>2</sub> as the redox probe	amperom.	0.001–20 ng·mL <sup>−1</sup>	0.2 pg·mL <sup>−1</sup>	serum	[34]
AuNPs/SnO <sub>2</sub> /rGO/GCE	PdNPs-V <sub>2</sub> O <sub>5</sub> /MWCNTs	CEA	Sandwich with immobilized anti-CEA and Ab <sub>2</sub> -label. H <sub>2</sub> O <sub>2</sub> as the redox probe	amperom.	0.0005–25 ng·mL <sup>−1</sup>	0.17 pg·mL <sup>−1</sup>	spiked serum	[35]
AuNPs/GCE	Pb@AuNPs@MWCNTs-Fe <sub>3</sub> O <sub>4</sub>	AFP	Sandwich with immobilized anti-AFP and Ab <sub>2</sub> -label. H <sub>2</sub> O <sub>2</sub> as the redox probe	amperom.	10 fg·mL <sup>−1</sup> – 100 ng·mL <sup>−1</sup>	3.33 fg·mL <sup>−1</sup>	spiked serum	[36]
β-CD/graphene/GCE	Pt@CuO/MWCNTs	AFP	Sandwich with immobilized anti-AFP and Ab <sub>2</sub> -label. H <sub>2</sub> O <sub>2</sub> as the redox probe	amperom.	0.001–20 ng·mL <sup>−1</sup>	0.33 pg·mL <sup>−1</sup>	spiked serum	[37]
AuNPs/Chit/GCE	MnO <sub>2</sub> /MWCNTs	AFP	Sandwich with immobilized anti-AFP and Ab <sub>2</sub> -label. H <sub>2</sub> O <sub>2</sub> as the redox probe	LSV	0.2–100 ng·mL <sup>−1</sup>	40 pg·mL <sup>−1</sup>	spiked plasma	[38]
AuNPs/MPTS/DpAu/GCE	AuNPs/PDDA/MWCNTs	AFP	Sandwich with immobilized anti-AFP and HRP/THI-Ab <sub>2</sub> -label. H <sub>2</sub> O <sub>2</sub> as the redox probe.	DPV	0.01–50 ng·mL <sup>−1</sup>	3 pg·mL <sup>−1</sup>	spiked serum	[39]
AuNPs/GCE	NiCoBP-MWCNTs	PSA	Sandwich with immobilized anti-PSA and Ab <sub>2</sub> -label. Glucose as the redox probe.	DPV	0.1–50 ng·mL <sup>−1</sup>	0.035 ng·mL <sup>−1</sup>	serum	[40]
Chit/TiO <sub>2</sub> /GCE	PB/MWCNTs/AuNPs	HCG	Sandwich with immobilized anti-HCG and HRP-Ab <sub>2</sub> -label. H <sub>2</sub> O <sub>2</sub> as the redox probe	DPV	0.05–150 mIU·mL <sup>−1</sup>	0.023 mIU·mL <sup>−1</sup>	Serum urine	[41]
p-DBP-AuNPs/GCE	Hyd-MWCNT(AuNP)	neomycin (Neo)	Sandwich with immobilized anti-Neo and Ab <sub>2</sub> -label. H <sub>2</sub> O <sub>2</sub> as the redox probe	amperom.	10–250 ng·mL <sup>−1</sup>	6.76 ± 0.17 ng·mL <sup>−1</sup>	meat	[42]
PAMAM/AuNPs/Chit/GCE	HRP-MWCNTs	<i>E. coli</i>	Sandwich with immobilized anti- <i>E. coli</i> and Ab <sub>2</sub> -label. ANI + H <sub>2</sub> O <sub>2</sub> to give PANI as the redox probe	DPV	10 <sup>−2</sup> –10 <sup>−6</sup> cfu·mL <sup>−1</sup>	50 cfu·mL <sup>−1</sup>	milk, yogur	[43]
AuNPs/GCE/SPCE	PdNPs/MWCNTs	hIgG	Sandwich with immobilized RaHIgG and Ab <sub>2</sub> -label. Dissolved O <sub>2</sub> as the redox probe.	DPV	0.050–10 ng·mL <sup>−1</sup>	44 pg·mL <sup>−1</sup>	spiked serum	[44]

**Abbreviations:** ANI, aniline; APTES, 3-aminopropyltriethoxysilane; CEA, carcinoembryonic acid; Chit, chitosan; ConA, concavalin A; DpAu, porous deposited gold nanocrystal; fSWCNTs, forest SWCNTs; GA, glutaraldehyde; Hyd, hydrazine; L-Cys, L-cysteine; mIU: milli-international units; MPTS, 3-mercaptopropyl trimethoxysilane, PAMAM, polyamidoamine; p-DBP, poly-[2,5-di-(2-thienyl)-1H-pyrrole-1-(p-benzoic acid)]; pANI, poly(aniline); PDDA, Poly(diallyldimethylammonium); PG, pyrolytic graphite; RaHIgG, rabbit anti-human IgG antibody; THI, thionine.

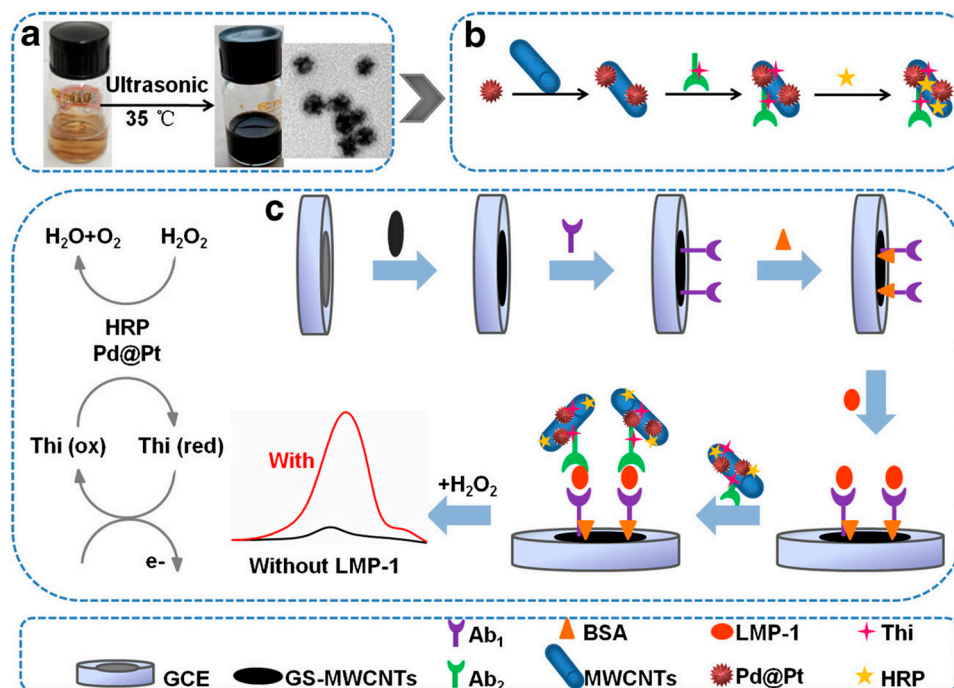


**Figure 6.** (a) Photographs of solutions before and after the reaction; (b) preparation of Ab<sub>2</sub>/Thi/HRP/Pd@Pt-MWCNTs; (c) fabrication procedure for LMP-1 immunosensor and DPV detection. Reprinted from [28] with permission.

Nanostructures combining CNTs with electroactive metals are attractive because of the relatively low cost of functionalization and high electrocatalytic effects. Therefore, preparation of labels for immunosensing using CNTs-metal nanoparticles hybrids has an increasing interest. Herein, the synthesis of nanoparticles in a variety of morphologies, and the use of single metals or combinations with other elements, represent some explored strategies. In an interesting example, amino-functionalized MWCNTs were used to attach PdPt nanocages with hollow interiors and porous walls to prepare active labels for signal amplification in an immunosensor for CEA (Figure 7). In this design, bimetallic PdPt nanoparticles exhibited intense catalytic effects toward the electrochemical reduction of H<sub>2</sub>O<sub>2</sub> and, furthermore, the configuration of hollow nanocages affording more exposed active sites reinforced this effect. Moreover, the high ability of CNTs to introduce numerous active nanoparticles leads to a high sensitivity, with a limit of detection of 0.2 pg·mL<sup>−1</sup> CEA, and enhances the immunosensor response. To complete the amplification scheme, the primary antibody was immobilized onto a 3-aminopropyltriethoxysilane (APTES) functionalized graphene sheets-GCE with high electron transfer efficiency [34].

PdNPs–vanadium pentoxide (V<sub>2</sub>O<sub>5</sub>)/MWCNTs hybrids were also used as labels for secondary antibodies (Ab<sub>2</sub>) in the preparation of another immunosensor for CEA. V<sub>2</sub>O<sub>5</sub>, acting as a catalyst, was stabilized by incorporation onto MWCNTs, and PdNPs, characterized by the high surface-to-volume ratio and high surface energy. It also rendered enhanced catalytic activity. Thus, the loading of PdNPs on the surface of V<sub>2</sub>O<sub>5</sub>/MWCNTs provided a label composite showing a synergetic behavior that remarkably improved the electrocatalytic activity towards the reduction of H<sub>2</sub>O<sub>2</sub>. This allowed a sandwich-type configuration to be constructed with the capture antibody immobilized onto a AuNPs/SnO<sub>2</sub>/rGO modified GCE and amperometric detection of CEA with a LOD as low as 0.17 pg·mL<sup>−1</sup> [35].

AFP is recognized as the reference tumor marker for hepatocellular carcinoma since its levels enhanced to a certain level (>10 ng·mL<sup>−1</sup>) in serum of patients [45]. An interesting electrochemical immunosensor for the determination of AFP in serum is the configuration developed by

Li et al. [36] where secondary antibodies are immobilized onto amplification labels composed of AuNPs-functionalized magnetic carbon nanotubes (MWCNTs-Fe<sub>3</sub>O<sub>4</sub>) with adsorbed lead ions. The presence of AuNPs facilitates the immobilization of the immunoreagent also increasing the electrochemical response, and the resulting nanocomposite (Pb<sup>2+</sup>@AuNPs@MWCNTs-Fe<sub>3</sub>O<sub>4</sub>), with a large surface area and high conductivity, showed an intense activity for the electrocatalytic reduction of H<sub>2</sub>O<sub>2</sub>. This same group also combined PtNPs, CuO and MWCNTs to form a label with catalytic activity toward H<sub>2</sub>O<sub>2</sub> [37]. In both cases, the detection of AFP at clinical levels could be performed by sandwich type immunoassays using highly conducting electrode platforms for immobilization of the capture antibody. Other electrochemical immunosensors for AFP have been also reported (Table 1) using amplification labels consisting of MnO<sub>2</sub>/MWCNTs nanocomposites [38], or AuNPs/poly-diallyldimethyl-ammonium (PDDA)/MWCNTs hybrids [39] for the respective binding of anti-AFP and HRP/THI-anti-AFP secondary antibodies and the detection of H<sub>2</sub>O<sub>2</sub> at AuNPs-modified GCEs after sandwich immunoassays.

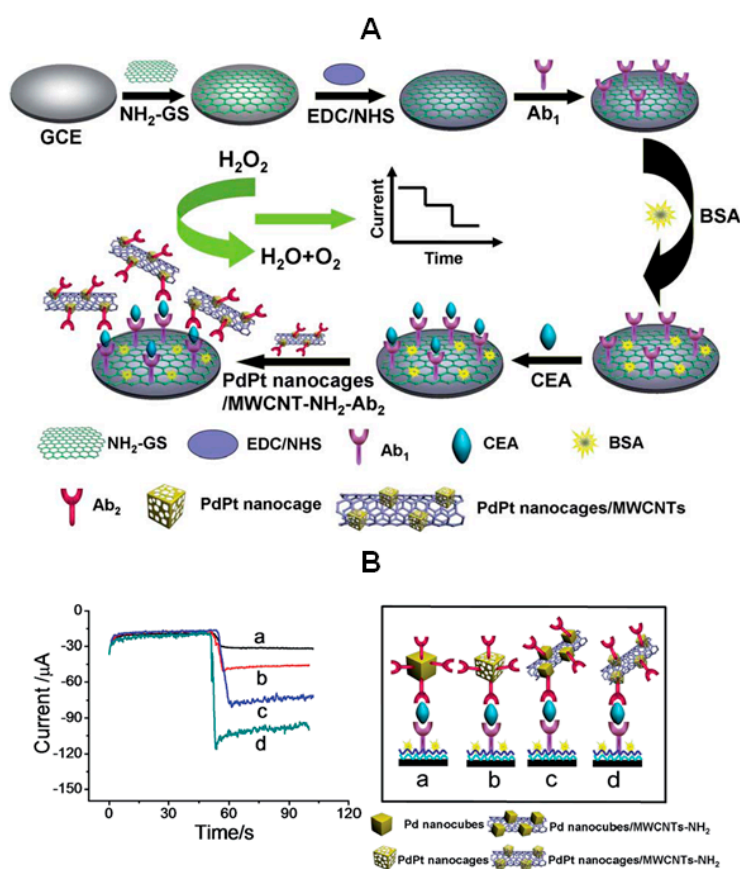


**Figure 7.** (A) Schematic illustration of the sandwich-type electrochemical immunosensor for carcinoembryonic antigen (CEA) using amino-functionalized multi-walled carbon nanotubes (MWCNTs) modified with PdPt nanocages with hollow interiors and porous walls as labels: Ab<sub>1</sub> immobilization on GCE modified with amine-functionalized graphene sheets (NH<sub>2</sub>-GS) and amperometric detection by addition of H<sub>2</sub>O<sub>2</sub> onto the PdPt/MWCNTs-Ab<sub>2</sub>-CEA-Ab<sub>1</sub>/graphene/GCE immunosensor; (B) Amperometric responses obtained with the developed immunosensor for the detection of 4 ng·mL<sup>-1</sup> of CEA using different signal labels: Pd nanocubes (a), PdPt nanocages (b), Pd nanocubes/MWCNT-NH<sub>2</sub> (c) and PdPt nanocages/MWCNT-NH<sub>2</sub> (d). Reprinted and adapted from [34] with permission.

Prussian Blue (PB) has been widely used as a mediator in electrochemical biosensors because of its high electronic catalytic activity and stability among other properties [46]. With the objective



of determining human chorionic gonadotropin (hCG) in serum and urine, an electrochemical immunosensor with signal amplification was constructed involving PB/MWCNTs composites. Chitosan was used for preventing PB leakage and to adsorb AuNPs which were further used to immobilize HRP-Ab<sub>2</sub>. A high sensitivity was attained by DPV detection of H<sub>2</sub>O<sub>2</sub> [41]. The electrochemical properties of Ni-MWCNTs composites could be improved by doping with cobalt and further addition of boron and phosphate. The resulting NiCoBP-MWCNTs showed outstanding electrocatalytic behavior for glucose oxidation. This behavior was exploited for the preparation of a label-free immunosensor for PSA where the hybrid was used to immobilize the detection antibody and as a mimic of glucose oxidase. The prepared sandwich immunosensor showed no interferences neither changes in assay conditions during the signal generation step [40]. A palladium nanoparticle decorated carbon nanotubes (PdNPs-MWCNTs) hybrid was designed as a label for the preparation of a disposable immunosensor for human IgG taking advantage of the label electrocatalytic activity towards dissolved oxygen [44]. A simple electrochemical tag consisted of an AuNPs/MWCNTs hydrazine conjugate with attached signal antibody was also synthesized for the sensitive detection of neomycin (Neo), an aminoglycoside effective against a variety of bacteria but nephrotoxic. An electrochemical immunosensor involving covalent immobilization of anti-Neo capture antibody onto a GCE modified with AuNPs and poly-[2,5-di-(2-thienyl)-1H-pyrrole-1-(p-benzoic acid)] (pDBP) was developed using sandwich immunoassay and amperometric detection at −0.5 V vs. Ag/AgCl after addition of H<sub>2</sub>O<sub>2</sub>. Hydrazine exhibited high ability to catalyze the electrochemical reduction of H<sub>2</sub>O<sub>2</sub> and, compared with enzymes, its use is easier and it is much less expensive. Furthermore, in this configuration, the multiple hydrazine molecules present on the label composite allowed a highly sensitive determination with a LOD lower than 7 ng·mL<sup>−1</sup> [42]. Finally, a sensitive immunosensor was also proposed for sensitive detection of *Escherichia coli* based on voltammetric measurement of PANI catalytically electrodeposited. The electrode platform was prepared using PAMAM dendrimer with encapsulated AuNPs that increased the amount of capture antibody immobilized and also accelerated the electron transfer process. Furthermore, the nanoprobe for signal amplification involved immobilization of the signal antibody onto MWCNTs and multiple HRP that catalyzed the oxidation of aniline to produce electroactive PANI on the immunosensor surface for the electrochemical detection. The developed method was applied to milk and other dairy products [43].

### 3.2. Graphene Used as Carrier for Signal Elements in Electrochemical Immunosensors

Graphene is a highly useful supporting material for electrochemical biosensing largely due to its unique properties already mentioned above. As the methods for obtaining graphene have progressed rapidly [47], currently, mechanical exfoliation, chemical and electrochemical reduction of graphene oxide (GO) to obtain the so-called reduced graphene oxide (rGO), or chemical vapor methods, are almost common procedures in laboratories. The large surface area, physiological stability, and good biocompatibility of graphene offer a comfortable environment for biomolecules immobilization. Thus, this nanomaterial can be used both to prepare highly sensitive platforms for electrochemical sensing with attached capture antibodies, or as well suited nanocarriers for signal amplification by immobilization of secondary antibodies and other elements.

Table 2 summarizes some relevant works regarding this latter purpose. As in the previous section, the most numerous applications of electrochemical immunosensors involving graphene tags as label-bearing nanocarriers are devoted to the detection of tumor biomarkers. An interesting example is the electrochemical immunosensor for the detection of squamous cell carcinoma antigen (SCCA) recently developed by Liu et al. [48]. SCCA is a kind of TA-4 subtypes existing at low level in normal epithelial cells but over-expressed in the epithelia of cancerous tissue. Since the amount of SCCA increases along with the incidence of cervical squamous cell carcinoma (CSCC), SCCA is well recognized as the tumor marker for CSCC [49]. As a novelty for the construction of a sandwich-type configuration, a sensing platform was prepared where  $\beta$ -cyclodextrin ( $\beta$ -CD) was

introduced into graphene oxide (GO) before it was fully reduced. In the resulting CD-GR, the presence of cyclodextrin avoided the aggregation of GR nanosheets and promoted the immobilization of primary antibodies by host-guest interaction to form Ab<sub>1</sub>-β-CD inclusion complexes. Separately, a 3D-graphene architecture was synthesized via a solvothermal procedure with introduction of hollow ternary PtPdCu nanocubes and immobilization of secondary antibodies by metal-NH<sub>2</sub> interaction. The resulting label nanocarrier demonstrated a high electrocatalytic ability for the reduction of H<sub>2</sub>O<sub>2</sub>, and the developed immunosensor provided highly sensitive electrochemical responses with an extremely low LOD of 25 fg·mL<sup>-1</sup>. A recent configuration for the determination of CEA biomarker was constructed by Lai et al. [50] using amplified inhibition of current from Fc present in an AuNPs/Chit/Fc/SPCE scaffold with immobilized anti-CEA capture antibody. A signal nanoprobe was fabricated by covalent immobilization of Ab<sub>2</sub> onto HRP-GO and, after performing a sandwich immunoassay, the electrochemical response was obtained from the catalyzed oxidation of 4-chloro-1-naphtol mediated by HRP. This reaction produced an insoluble precipitate that slowed down the voltammetric signal of Fc in DPV. The decreases in current were proportional to the biomarker level through a wide linear range of over five orders of magnitude with a LOD value down to 0.54 pg·mL<sup>-1</sup>.

Tissue polypeptide antigen (TPA) is a protein produced and released by proliferating cells used as a tumor biomarker for monitoring the occurrence of some cancer types, such as breast cancer, ovarian carcinoma, squamous cell lung cancer, and oral squamous cell carcinoma [51,52]. An electrochemical immunosensor for the detection of TPA in human serum was developed using multifunctional graphene nanocomposites prepared with Fe<sub>3</sub>O<sub>4</sub> and AuNPs that exhibited synergetic electrocatalytic effects toward the reduction of H<sub>2</sub>O<sub>2</sub>. Under optimal conditions, the reported sandwich-type immunosensor exhibited a wide linear range from 10<sup>-5</sup> to 10<sup>2</sup> ng·mL<sup>-1</sup> with a low LOD of 7.5 fg·mL<sup>-1</sup> [53]. Human apurinic/aprimidinic endonuclease 1 (APE1) is a multifunctional protein in the DNA base excision repair pathway [54]. Elevated APE1 levels or altered subcellular localization in various types of cancer suggest a prognostic relevance, and the possible use of APE1 as biomarker for non-small cell lung cancer and other diseases. The detection of APE1 in biological samples requires highly sensitive sensors. With this purpose, an electrochemical immunosensor was constructed employing a GCE platform modified with graphene and gold nanochains (AuNCs) where anti-APE1 capture antibody was immobilized. Furthermore, a signal carrier for attachment of Fc-labeled secondary antibody (Fc-Ab<sub>2</sub>) and ALP was also prepared with the ionic liquid 1-butyl-3-methylimidazolium tetra-fluoroborate (IL) and AuNPs adsorbed also onto graphene. This composite could significantly enhance the sensitivity and promote the electron transfer. Once a sandwich-type configuration was established, the addition of ascorbic acid 2-phosphate (AA-p) as the enzyme substrate started a cascade of catalytic reactions where the electrochemical oxidation of the ascorbic acid obtained in the presence of ALP was catalyzed by the Fc/Fc<sup>+</sup> system to further enhance the current response [55]. This immunosensor exhibited a linear response between 0.1 and 80 pg·mL<sup>-1</sup> APE1 and a LOD of 0.04 pg·mL<sup>-1</sup>.

**Table 2.** Electrochemical immunosensors using graphene nanomaterials as labels.

Electrode	Label	Analyte	Immunoassay	Technique	Linear Range	LOD	Sample	Reference
$\beta$ -CD-graphene/GCE	Pt/PdCu-3DGR	SCCA	Sandwich with immobilized anti-SCCA and Ab <sub>2</sub> -label. H <sub>2</sub> O <sub>2</sub> as the redox probe	amperom.	$0.0001\text{--}1\text{ ng}\cdot\text{mL}^{-1}$ $1\text{--}30\text{ ng}\cdot\text{mL}^{-1}$	$25\text{ fg}\cdot\text{mL}^{-1}$	serum	[48]
AuNPs/Chit-Fc/SPCE	HRP-GO	CEA	Sandwich with immobilized anti-CEA and Ab <sub>2</sub> -label. H <sub>2</sub> O <sub>2</sub> /4-Cl-1-naphtol as the redox probe	DPV	$0.001\text{--}100\text{ ng}\cdot\text{mL}^{-1}$	$0.54\text{ pg}\cdot\text{mL}^{-1}$	serum	[50]
AuNPs/GCE	Fe <sub>3</sub> O <sub>4</sub> /AuNPs/graphene	TPA	Sandwich with immobilized anti-TPA and Ab <sub>2</sub> -label. H <sub>2</sub> O <sub>2</sub> as the redox probe	amperom.	$10^{-5}\text{--}100\text{ ng}\cdot\text{mL}^{-1}$	$7.5\text{ fg}\cdot\text{mL}^{-1}$	spiked serum	[53]
AuNCs/graphene/GCE	AP/AuNPs/IL/pSS/graphene	APE1	Sandwich with immobilized anti-APE1 and Fc-Ab <sub>2</sub> -label. AA-p as enzyme substrate.	CV	$1\text{--}80\text{ pg}\cdot\text{mL}^{-1}$	$0.04\text{ pg}\cdot\text{mL}^{-1}$	spiked serum	[55]
AuNWs/GO/SPCE	CuS/GO	AFP	Sandwich with immobilized anti-AFP and Ab <sub>2</sub> -label. H <sub>2</sub> O <sub>2</sub> as the redox probe	amperom.	$0.001\text{--}10\text{ ng}\cdot\text{mL}^{-1}$	$0.5\text{ pg}\cdot\text{mL}^{-1}$	serum	[56]
IL/rGO/GA/GCE	IL/rGO/PDDA/PB/AuNPs	AFP	Sandwich with immobilized anti-AFP and Ab <sub>2</sub> -label. H <sub>2</sub> O <sub>2</sub> as the redox probe	SWV	$0.01\text{--}100\text{ ng}\cdot\text{mL}^{-1}$	$4.6\text{ pg}\cdot\text{mL}^{-1}$	serum	[57]
AuNPs/GCE	graphene-PAMAM	AFP	Sandwich with immobilized anti-AFP and HRP-Ab <sub>2</sub> -label. H <sub>2</sub> O <sub>2</sub> + HQ as the redox probe	CV	$1.0\text{--}100\text{ ng}\cdot\text{mL}^{-1}$	$0.45\text{ ng}\cdot\text{mL}^{-1}$	serum	[58]
AuNPs/MWCNTs-SO <sub>3</sub> H/GCE	MPd@PtNPs/NH <sub>2</sub> -graphene	PSA	Sandwich with immobilized anti-PSA and Ab <sub>2</sub> -label. H <sub>2</sub> O <sub>2</sub> as the redox probe	amperom.	$10^{-5}\text{--}50\text{ ng}\cdot\text{mL}^{-1}$	$3.3\text{ fg}\cdot\text{mL}^{-1}$	serum	[59]
Chit-AuNPs/GCE	cGS-TB cGS-PB	CEA AFP	Multiplex sandwich with immobilized anti-CEA or anti-AFP and each Ab <sub>2</sub> -label. TB or PB as redox probes	DPV	$0.5\text{--}60\text{ ng}\cdot\text{mL}^{-1}$	$0.1\text{ ng}\cdot\text{mL}^{-1}$ $0.05\text{ ng}\cdot\text{mL}^{-1}$	serum	[60]
AuNPs/GCE	PtNPs/PEI/GOx/HRP/GO	CEA AFP	Multiplex sandwich with immobilized anti-CEA or anti-AFP and THI-anti-CEA-label or Fc-anti-AFP-label. Glucose as the redox probe	SWV	$0.01\text{--}100\text{ ng}\cdot\text{mL}^{-1}$	$1.64\text{ pg}\cdot\text{mL}^{-1}$ $1.33\text{ pg}\cdot\text{mL}^{-1}$	serum	[61]
ZnO NR/rGO/PWE	rGO/Ag@BSA	HCG, PSA CEA	Multiplex sandwich with immobilized anti-PSA or anti-CEA and each Ab <sub>2</sub> -label. H <sub>2</sub> O <sub>2</sub> as the redox probe	amperom.	$0.002\text{--}120\text{ mIU}\cdot\text{mL}^{-1}$ $0.001\text{--}110\text{ ng}\cdot\text{mL}^{-1}$ $0.001\text{--}100\text{ ng}\cdot\text{mL}^{-1}$	$0.0007\text{ mIU}\cdot\text{mL}^{-1}$ $0.35\text{ pg}\cdot\text{mL}^{-1}$ $0.33\text{ pg}\cdot\text{mL}^{-1}$	serum	[62]
Protein A/Nafion/GCE	PTCA/AuNPs/rGO	AFP CEA SS2	Multiplex sandwich with immobilized anti-AFP, anti-CEA or anti-SS2 and THI-anti-AFP-label, Co(bpy) <sub>3</sub> <sup>3+</sup> -anti-CEA-label, or Fc-anti-SS2-label	DPV	$0.016\text{--}50\text{ ng}\cdot\text{mL}^{-1}$ $0.010\text{--}50\text{ ng}\cdot\text{mL}^{-1}$ $0.012\text{--}50\text{ ng}\cdot\text{mL}^{-1}$	$5.4\text{ pg}\cdot\text{mL}^{-1}$ $2.8\text{ pg}\cdot\text{mL}^{-1}$ $4.2\text{ pg}\cdot\text{mL}^{-1}$	-	[63]
AuNPs@BSA/GCE	rGO/TEPA-Pb <sup>2+</sup> rGO/TEPA-Cu <sup>2+</sup>	hs-CRP sCD40	Multiplex sandwich with immobilized anti-CRP or anti-CD40 and each Ab <sub>2</sub> -label. Pb <sup>2+</sup> or Cu <sup>2+</sup> as redox probes	DPV	$0.5\text{--}100\text{ ng}\cdot\text{mL}^{-1}$	$16.7\text{ pg}\cdot\text{mL}^{-1}$ $13.1\text{ pg}\cdot\text{mL}^{-1}$	serum	[64]
AuNPs(GCE)	AP/PtNPs/CeO <sub>2</sub> /GO	influenza	Sandwich with immobilized anti-influenza and Ab <sub>2</sub> -label. 1-naphtol as the redox probe.	DPV	$0.001\text{--}1.0\text{ ng/mL}$ $1.0\text{--}500\text{ ng}\cdot\text{mL}^{-1}$	$0.43\text{ pg}\cdot\text{mL}^{-1}$	spiked serum	[65]
AuNPs/PB/PANI/pAA/GCE	AuNPs/Chit/graphene	SAL	Indirect competitive with immobilized SAL, anti-SAL and HRP-Ab <sub>2</sub> -label. H <sub>2</sub> O <sub>2</sub> as the redox probe	CV	$0.08\text{--}1000\text{ ng}\cdot\text{mL}^{-1}$	$0.04\text{ ng}\cdot\text{mL}^{-1}$	feed, pork	[66]
AuNPs/PAMAM/PANI/graphene/GCE	HRP-GO	Estradiol (EE2)	Indirect competitive with immobilized EE2 and anti-EE2-label. H <sub>2</sub> O <sub>2</sub> + HQ as the redox probe	DPV	$0.04\text{--}7.0\text{ ng}\cdot\text{mL}^{-1}$	$0.02\text{ ng}\cdot\text{mL}^{-1}$	tap water, milk	[67]
MWCNTs/PB/Chit/GA/GCE	HRP/GO	<i>Clostr. difficile</i> toxinB (TcdB)	Sandwich with immobilized anti-TcdB and HRP-Ab <sub>2</sub> -label. H <sub>2</sub> O <sub>2</sub> as the redox probe	DPV	$0.003\text{--}320\text{ ng}\cdot\text{mL}^{-1}$	$0.7\text{ pg}\cdot\text{mL}^{-1}$	human stool	[68]

**Abbreviations:** AA-p, ascorbic acid 2-phosphate; ALP, alkaline phosphatase; APE1, Human apurinic/apyrimidinic endonuclease 1; AuNWs, gold nanowires functionalized graphene oxide; CEA, carcinoembryonic acid; cGS, carboxyl graphene nanosheets; Chit, chitosan; GA, glutaraldehyde; GR, graphene; IL, ionic liquid; mIU: milli-international units; MPd@PtNPs, mesoporous core-shell Pd@Pt nanoparticles; PAA, polyacrylamide; PANI, polyaniline; PB, Prussian blue; PDDA, polydiallyl dimetilammonium; PTCA, 3,4,10-perylene tetracarboxylic acid; PWE, pape working electrode; SS2, *streptococcus suis* serotype 2; TB, toluidin blue; THI, thionine; TPA, tissue polypeptide antigen.

An enzyme-free and all-electrochemical immunosensor was proposed for the detection of the oncofetal glycoprotein AFP. Ultra-thin gold nanowires functionalized graphene oxide (AuNWs/GO) were prepared and used as an electrochemical signal platform. Furthermore, CuS/GO composites with covalently immobilized AFP-secondary antibodies ( $Ab_2$ ) were also fabricated and employed as the electrochemical bioprobe for detection of the biomarker by sandwich immunoassay. The developed configuration was mounted onto a 3D paper-based analytical device (3D- $\mu$ PECI) comprised of three SPEs acting as the counter, reference and working electrodes. The catalytic activity of CuS on the  $H_2O_2$  electrochemical process provided efficient amperometric responses and a good sensitivity for the determination of AFP in serum [56]. This inexpensive and portable 3D paper-based immunosensor provided a wide calibration range ( $0.001\text{--}10\text{ ng}\cdot\text{mL}^{-1}$ ) and a low LOD ( $0.5\text{ pg}\cdot\text{mL}^{-1}$ ) and was successfully applied to the determination in serum samples from both healthy people and cancer patients. A nanocomposite involving PDDA protected-PB/AuNPs and the ionic liquid 1-aminopropyl-3-methylimidazoliumchloride (IL) was fabricated to prepare another electrochemical immunosensor for AFP. IL-rGO was used as electrode modifier to capture a large amount of anti-AFP capture antibodies. Then, the catalytic reaction between  $H_2O_2$  and the IL-rGO-Au-PDDA-PB- $Ab_2$  nanocomposite enhanced the signal response [57]. Good results were also obtained by Shen et al. [58] in the development of a sensitive amperometric immunosensor for AFP using a dendrimer functionalized-graphene as nanocarrier for HRP-labeled secondary antibodies. In this case, the high efficiency of PAMAM (G 4.0) for the covalent immobilization of  $Ab_2$  combined with the ability of graphene to accelerate the electron transfer enhancing the amperometric responses, allowed a fast response and a sensitive method (linear range of  $1.0\text{--}100\text{ ng}\cdot\text{mL}^{-1}$  and LOD of  $0.45\text{ ng}\cdot\text{mL}^{-1}$ ) for application to biological samples.

As occurred with CNTs, the combination of metal nanoparticles and graphene is a useful alternative in the preparation of labels for signal amplification. In order to decrease the costs and retain the catalytic efficiency of these nanoparticles, and to obtain hybrids with better electronic properties, diverse morphologies and/or blending of different metals and oxides have been employed. Very recently, mesoporous core-shell Pd@Pt NPs/amino group functionalized graphene nanocomposites were used for development of an ultrasensitive sandwich-type electrochemical immunosensor for PSA. The method implied a dual signal amplification strategy provided (a) by sulfo group-functionalized MWCNTs used as substrate material to enhance GCE conductivity and AuNPs enhancing the loading of primary antibodies; and (b) the nanocarriers for immobilization of  $Ab_2$  prepared with amino group-functionalized graphene and Pd@Pt NPs providing high specific surface area, biocompatibility, and electrocatalytic activity towards the reduction of  $H_2O_2$  [59]. Various multiplexed configurations for the simultaneous detection of cancer biomarkers using graphene-based nanocarriers for signal amplification have also been developed. For example, CEA and AFP were determined using a sandwich-type immunoassay involving immobilization of capture antibodies onto Chit-AuNPs/GCE and carboxyl graphene nanosheets (CGS) employed as immunosensing probes with anti-CEA or anti-AFP secondary antibodies immobilized respectively onto toluidine blue or Prussian blue (Figure 8). The authors synthesized CGS-PB and CGS-TB nanocomposites from commercial CGS (obtained from JCNANO, Nanjing, China). DPV responses of these electroactive labels were used for the sensitive and selective electrochemical detection providing LODs of  $0.05$  and  $0.1\text{ ng}\cdot\text{mL}^{-1}$  for AFP and CEA determination, respectively [60]. Similarly, Jia et al. [61] developed another configuration for the same markers. In this case, graphene was modified with platinum nanoparticles and the enzymes GOx and HRP, whereas thionine and Fc were used to label anti-CEA and anti-AFP  $Ab_2$ , respectively. Greatly enhanced sensitivity resulted from using this signal amplification strategy for the determination of both cancer biomarkers in a single run (working range of  $0.01\text{--}100\text{ ng}\cdot\text{mL}^{-1}$ ), reaching LODs of  $1.33$  for AFP and  $1.64\text{ pg}\cdot\text{mL}^{-1}$  for CEA.

Paper working electrodes (PWEs) prepared with reduced graphene oxide (rGO-PWEs) have great potential to be widely used to construct electrochemical immunosensors because of their simple fabrication, portability, and low cost. Using ZnO nanorods (ZnONR), ZnONR/rGO-PWEs

sensor platforms were employed to immobilize the specific capture antibodies, and thus, the challenge of preparing a multiple immunoassay configuration for the simultaneous determination of three biomarkers, CEA, PSA and hCG was achieved. ZNORs provided abundant sites for capture probes binding and, furthermore, rGO/Ag@BSA composites, combining the large surface area of rGO and high catalytic activity of Ag@BSA nanoparticles toward  $\text{H}_2\text{O}_2$  reduction, were excellent signal labels for response amplification. The current generated from the reduction of  $\text{H}_2\text{O}_2$  and further amplified by signal labels-promoted deposition of silver, making possible the simultaneous determination of the three markers without cross-reactivity and a suitable sensitivity, with LOD values of  $0.0007 \text{ mIU} \cdot \text{mL}^{-1}$  (CEA),  $0.35 \text{ pg} \cdot \text{mL}^{-1}$  (PSA), and  $0.33 \text{ pg} \cdot \text{mL}^{-1}$  (hGH), and allowed the successful application of the immunosensor to clinical samples [61]. Dual functionalized graphene sheets integrated with redox probes were also utilized for the construction of an amperometric immunosensor for simultaneous detection of other three analytes, AFP, CEA, and *Streptococcus suis* serotype 2 (SS2). Using a sandwich-type amperometric assay, three specific antibodies were immobilized onto protein A/Nafion modified GCE, and the corresponding detection antibodies were firstly linked with the respective three redox-probes (thionine,  $\text{Co}(\text{bpy})_3^{3+}$  or ferrocene), and further integrated to a 3,4,9,10-perylene tetracarboxylic acid (PTCA)/AuNPs/GS nanocomposite through AuNPs and carboxyl group, and employed as the tracer [63].

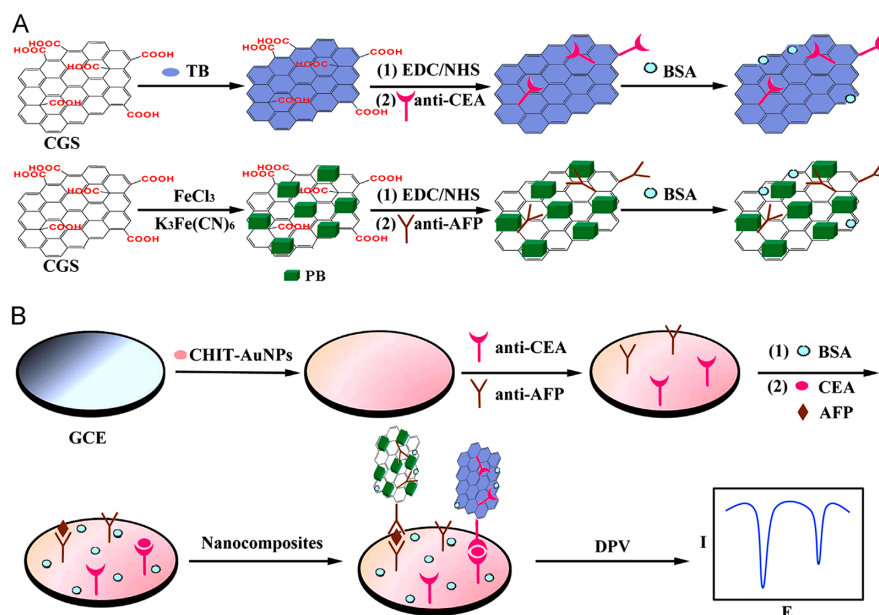


**Figure 8.** Schematic illustration of: (A) the preparation of biofunctional carboxyl graphene nanosheets (CGS) nanocomposites with toluidine blue (TB) or Prussian blue prepared from  $\text{FeCl}_3$  and  $\text{K}_3\text{Fe}(\text{CN})_6$  and (B) the multiplexed electrochemical immunoassay protocol for determination of CEA and  $\alpha$ -fetoprotein (AFP). Reprinted from [60] with permission.

Several biomarkers are associated with an increased risk of cardiovascular disease (CVD). Examples are high-sensitive C-reactive protein (hsCRP) for acute myocardial infarction, and soluble CD40 ligand (sCD40L) involved in thrombus stabilization and platelet activation [69]. The detection of these compounds at clinically significant concentrations is particularly important for the early diagnosis of CVD. Yuan et al. [64] developed a multiplex electrochemical immunosensor for the simultaneous determination of hsCRP and sCD40L using a signal amplification strategy that involved the adsorption of lead and copper metal ions and the respective detection antibodies ( $\text{Ab}_2$ ) onto rGO/tetraethylene pentamine (TEPA) platforms. This nanomaterial possesses a high number of amino groups that facilitate the interaction with metal ions and further immobilization of  $\text{Ab}_2$ . A sandwich type immunoassay was performed with the capture antibodies immobilized onto a GCE modified



with AuNPs@BSA. DPV measurements of the peak currents of  $\text{Pb}^{2+}$  and  $\text{Cu}^{2+}$  in the corresponding anti-hsCRP-rGO/TEPA- $\text{Pb}^{2+}$  and anti-sCD40L-rGO/TEPA- $\text{Cu}^{2+}$  provided a wide linear range from 0.5 to 100  $\text{ng}\cdot\text{mL}^{-1}$ .

Cerium oxide nanoparticles  $\text{CeO}_2$  ( $\text{CeO}_2\text{NPs}$ ) have been widely applied in the preparation of electrochemical biosensors because of their catalytic and free radical scavenging properties. However,  $\text{CeO}_2\text{NPs}$  have low electron conductivity. To overcome this shortcoming, other nanomaterials such as graphene, highly conductive and with large specific surface area, can be used as a matrix for  $\text{CeO}_2\text{NPs}$  loading, this improving their stability and electrocatalytic ability. In a recent article, Yang et al. [65] prepared an electrochemical immunosensor for influenza antigen using PtNPs/ $\text{CeO}_2\text{NPs}$ /GO composites as signal amplifiers with immobilized secondary antibodies and alkaline phosphatase (ALP) (Figure 9). 1-naphthylphosphate was used as the enzyme substrate to form 1-naphthol which was detected at  $\text{Ab}_1$ -AuPdNPs/GCE by cyclic voltammetry.

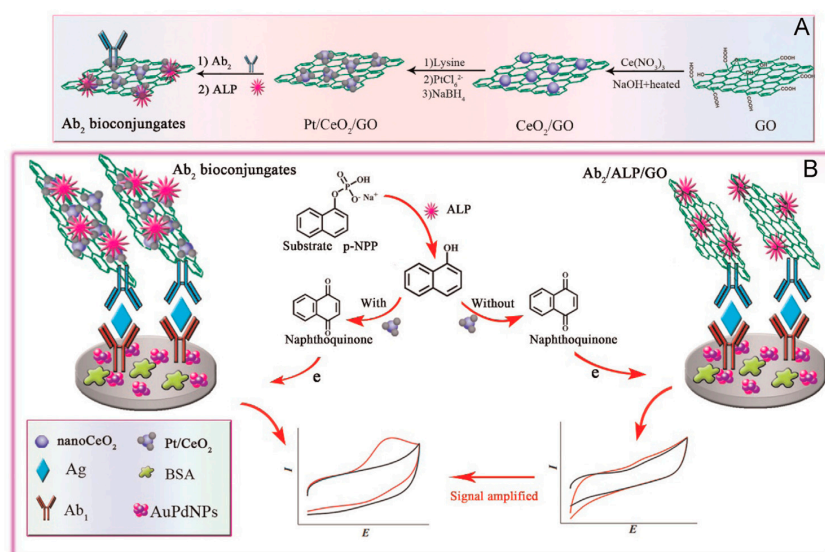


**Figure 9.** Schematic illustration of: (A) the step wise preparation procedure of PtNPs/ $\text{CeO}_2\text{NPs}$ /GO composites used as signal probes and (B) the amplification mechanism of detection signal at an  $\text{Ab}_1$ -AuPdNPs/GCE: ALP catalyzes the dephosphorylation of 1-NPP substrate giving naphthoquinone which is electrochemically reduced onto the immunosensor prepared with  $\text{Ab}_2$ /ALP/PtNPs/ $\text{CeO}_2\text{NPs}$ /GO (current amplification) or  $\text{Ab}_2$ /ALP/GO (no amplification). Cyclic voltammograms in absence (black) and in the presence (red) of antigen (Ag). Reprinted from [65] with permission.

Electrochemical immunosensors with graphene-based tags for signal amplification have also been applied to the determination of drugs residues in food samples. An illustrative example is the work by Huang et al. [66] for the determination of salbutamol (SAL), a  $\beta_2$ -adrenergic receptor used for humans and in veterinary medicine whose residues in meat can be toxic [70]. The detection of SAL at low concentration levels was accomplished by preparing an electrode scaffold by modification of a GCE with AuNPs, polyaniline/poly(acrylic acid) (PANI(PAA)), and Prussian blue. The antigen was immobilized onto the modified electrode to perform a competitive immunoassay, and a nanolabel with Chit-graphene as core and AuNPs as a shell was fabricated and used to conjugate HRP-anti-SAL antibody. The resulting immunosensor, with a wide linear range, from 0.08 to 1000  $\text{ng}\cdot\text{mL}^{-1}$ , and a low limit of detection, 0.04  $\text{ng}\cdot\text{mL}^{-1}$ , was applied to the analysis of swine feed and pork samples. The same group prepared an electrochemical immunosensor for estradiol which was applied to water and milk samples. In this case, graphene/PANI and poly(amidoamine) (PAMAM)/AuNPs composites were used as the transducer modifiers to improve the current response increasing the number of available binding sites for antigen immobilization. Moreover, HRP-GO conjugates were employed

as carriers for the anti-estradiol immobilization and construction of a competitive configuration [67]. *Clostridium difficile* toxin B (TcdB) is one of the primary contributing factors to the pathogenesis of *C. difficile*-associated diseases and is used as a biomarker in clinical diagnoses. A simple method for the determination of TcdB was developed by means of a sandwich-type electrochemical immunosensor. Greatly enhanced sensitivity was achieved (LOD of  $0.7 \text{ pg} \cdot \text{mL}^{-1}$ ) by fabricating the immunosensor using a layer-by-layer coated MWCNTs, PB, Chit and glutaraldehyde composite on the working electrode as well as HRP-graphene oxide as a nanocarrier in a multienzyme amplification strategy [68]. Moreover, this sensitive immunosensor provided satisfactory results in the analysis of real human stool samples.

### 3.3. Other Carbon Nanomaterials Used as Carriers for Signal Elements in Electrochemical Immunosensors

Besides the above-mentioned carbon nanomaterials, other carbon nanoforms have also demonstrated their suitability as tools for enhancing electrocatalytic ability and sensitivity of electrochemical immunoassays. As it can be seen in Table 3, these so-called uncommon carbon nanomaterials have also been employed in the design of nanotags for current amplification in a variety of immunosensors.

Single-walled carbon nanohorns (CNHs) consist of horn-shaped graphene sheets with a length of 40–50 nm and a diameter ranging between 2 and 5 nm [71]. CNHs assemble to form nanostructures similar to dahlia flowers composed of several units with a diameter near from 100 nm [72]. Synthesis of CNHs by vaporizing pure graphite rods via  $\text{CO}_2$  laser ablation without using any metal catalysts confers an important advantage of these materials, which can be used directly without post-treatment. The special properties of CNHs derive from the high conductivity, the large surface area, the high number of defects, and the amount of inner nanospaces. Zhu and Xu reviewed the general applications of carbon nanohorns [73].

Some examples have been published regarding the use of CNHs-hybrids as efficient tools to implement signal amplification strategies for immunosensing [74]. As an example, CNHs functionalized with two enzymes, HRP and glucose oxidase, were employed for the immobilization of a detection antibody for AFP and construction of a sandwich-type immunosensor involving the capture antibody immobilized onto a glassy carbon electrode modified with GR and AuNPs. Electrochemical impedance spectroscopy was used to obtain the analytical signals with  $\text{Fe}(\text{CN})_6^{3-/4-}$  as the redox probe. The responses were produced by biocatalyzed oxidation of 4-chloro-1-naphthol that generates an insulating precipitate (benzo-4-chlor-hexidine) resulting in an efficient blocking of the electrode surface [75]. Nanogold-enriched carbon nanohorns (AuNPs/CNHs) with immobilized anti-AFP antibodies were also utilized as trace tags for the electrochemical detection of AFP. Disposable screen-printed carbon electrodes modified with chitosan were used as electrochemical platforms for covalent immobilization of the capture antibody and construction of a sandwich immunoassay by conjugation with AuNPs/CNHs- $\text{Ab}_2$  [76]. The same group also proposed a dual immunosensor for AFP and CEA using Strept/AuNPs/CNHs hybrids prepared by in situ growth of nanogold on  $\text{COOH}$ -CNHs and further functionalization with streptavidin. Then, a sandwich-type immunoreaction was performed using Biotin- $\text{Ab}_2$  to capture the as prepared tags followed by silver deposition onto the immunoconjugates and recording of the stripping voltammetric responses [77]. In another original configuration, CNHs-hollow Pt chains (HPtCs) hybrid material was fabricated as a signal tag to label secondary antibodies in the development of an electrochemical immunosensor for procalcitonin (PCT), a diagnostic biomarker for septicemia. CNHs/HPtCs combined the advantages of CNHs with the high specific surface area and catalytic activity of HPtCs. Secondary PCT antibody conjugated with thionine and HRP was immobilized onto CNHs/HPtCs and a sandwich type configuration was implemented using PCT capture antibodies immobilized onto  $\text{rGO}/\text{AuNPs}$  nano-composite film. Using this strategy, the catalytic activity of HPtCs towards  $\text{H}_2\text{O}_2$  was enhanced by HRP for dual synergy amplification [78]. Another immunosensor for PCT was also developed by the same authors using PAMAM assembled to CNHs/HPtNPs in order to increase the amount of immobilized thionine [79].

**Table 3.** Electrochemical immunosensors using uncommon carbon nanostructures as labels.

Electrode	Label	Analyte	Immunoassay	Technique	Linear Range	LOD	Sample	Reference
AuNPs/rGO/GCE	HRP/GOx/CNHs	AFP	Sandwich with immobilized anti-AFP and Ab <sub>2</sub> -label. H <sub>2</sub> O <sub>2</sub> + 4-Cl-1-naphthol as the redox probe	EIS	0.001–60 ng·mL <sup>−1</sup>	0.33 pg·mL <sup>−1</sup>	spiked serum	[75]
Chit/SPCE	AuNPs/CNHs	AFP	Sandwich with immobilized anti-AFP and Ab <sub>2</sub> -label. Preoxidized Au as the redox probe	DPV	0.0001–1 ng·mL <sup>−1</sup>	0.07 pg·mL <sup>−1</sup>	serum	[76]
GA/Chit/SPCE	Strept/AuNPs/CNHs	AFP CEA	Multiplex sandwich with immobilized anti-AFP and anti-CEA and biotin-Ab <sub>2</sub> -label. Deposited AgNPs as the redox probe	LSSV	0.0001–1.0 pg·mL <sup>−1</sup>	$\frac{0.024 \text{ pg}\cdot\text{mL}^{-1}}{0.032 \text{ pg}\cdot\text{mL}^{-1}}$	serum	[77]
AuNPs/rGO/GCE	HPtCs/CNHs	PCT	Sandwich with immobilized anti-PCT and Ab <sub>2</sub> -label. H <sub>2</sub> O <sub>2</sub> as the redox probe	DPV	0.001–20 ng·mL <sup>−1</sup>	0.43 pg·mL <sup>−1</sup>	serum	[78]
AuNPs/GCE	HPtNPs-PAMAM-CNHs	PCT	Direct with immobilized THI-anti-PCT-label. H <sub>2</sub> O <sub>2</sub> as the redox probe	DPV	0.01–20 ng·mL <sup>−1</sup>	1.74 pg·mL <sup>−1</sup>	serum	[79]
AuNPs@MWCNTs/GCE	PtNP-Fc-NH <sub>2</sub> -C60	PCT	Sandwich with immobilized anti-PCT and GOx-Ab <sub>2</sub> -label. H <sub>2</sub> O <sub>2</sub> + glucose as the redox probe	DPV	0.01–10 ng·mL <sup>−1</sup>	6 pg·mL <sup>−1</sup>	serum	[80]
Protein A-AuNDs/GCE	PAMAM-C60	EPO	Sandwich with immobilized anti-EPO and Ab <sub>2</sub> -label. TOAB as booster of C60 electroactivity	DPV	0.01–80 mIU mL <sup>−1</sup>	0.0027 mIU·mL <sup>−1</sup>	serum	[81]
GQDs/GCE	Fe <sub>3</sub> O <sub>4</sub> @GQDs-Cu-apoferritin	ALVs-J	Sandwich with immobilized anti-ALVs-J and Ab <sub>2</sub> -label. Cu as the redox probe.	DPV	$\frac{10^{2.08} - 10^{4.50}}{\text{TCID}_{50}} \cdot \text{mL}^{-1}$	115 TCID <sub>50</sub> ·mL <sup>−1</sup>	-	[82]
MBs/SPCE	HRP-CNS	phospho-p53	Sandwich with immobilized anti-phospho-p53 and Ab <sub>2</sub> -label. H <sub>2</sub> O <sub>2</sub> + THI as the redox probe	SWV	0.01–5 ng·mL <sup>−1</sup>	3.3 pg·mL <sup>−1</sup>	-	[83]
Graphene/Chit/GCE	HRP-CNS	MC-LR	Sandwich with immobilized anti MC-LR and Ab <sub>2</sub> -label. H <sub>2</sub> O <sub>2</sub> as the redox probe	DPV	0.05–15 µg mL <sup>−1</sup>	0.016 µg mL <sup>−1</sup>	waters	[84]
Fe <sub>3</sub> O <sub>4</sub> /PANI/Nf/ITO	multi-HRP-HCS	BaP	Competitive indirect with immobilized BaP, anti-BaP and Ab <sub>2</sub> -label. H <sub>2</sub> O <sub>2</sub> + HQ as the redox probe	CV	0.008–2 nmol L <sup>−1</sup>	0.004 nmol L <sup>−1</sup>	spiked serum	[85]
PEG/SPCE	AuNPs/CNS	hIgG	Sandwich with anti-hIgG and Ab <sub>2</sub> -label. AuNPs + HCl as the redox probe	DPV	0.01–10 ng·mL <sup>−1</sup>	9 pg·mL <sup>−1</sup>	serum	[5]
AuNPs/SPCE	AuNPs/PDDA/PB/MCN/GOx	hIgG	Sandwich with anti-hIgG and Ab <sub>2</sub> -label. Glucose as the redox probe	DPV	0.01–100 ng·mL <sup>−1</sup>	<7.8 pg·mL <sup>−1</sup>	-	[6]
IL/rGO/pSS/GCE	AuNPs/C	CEA PSA AFP	Sandwich with immobilized anti-CEA, anti-PSA and THI-anti-CEA, DAP-anti-PSA and Cd <sup>2+</sup> -anti-AFP-label.	SWV	0.01–100 ng·mL <sup>−1</sup>	$\frac{2.7 \text{ pg}\cdot\text{mL}^{-1}}{4.8 \text{ pg}\cdot\text{mL}^{-1}}$ 3.1 pg·mL <sup>−1</sup>	serum	[86]

**Abbreviations:** ALVs-J, avian leukosis virus subgroup J; AuNcs, gold nanoclusters; AuNDs, gold nanodendrites; BaP, benzo[a]pyrene BBP, 3-bromobiphenyl; Chit, chitosan; CHNc, carbon hollow nanochain; CNHs, carbon nanohorns; DAP, 2,3-diaminophenazine; GQD, graphene quantum dots; GS, graphene sheet; HCS, highly carbonized nanospheres; IL, ionic liquid; mIU: milli-international units; MBs, magnetic beads; Nf, Nafion; PCT, prolactin; pDOP, polydopamine; pSS, poly(sodium-*p*-styrene sulfonate); OMC, ordered mesoporous carbon; PAMAM, polyamidoamine; PEG, polyethyleneglycol; rGO, reduced graphene oxide; TCID<sub>50</sub>, 50% Tissue Culture Infective Dose; THI, thionine; TOAB, tetraoctylammonium bromide.

Fullerene ( $C_{60}$ ) is the smallest stable and most abundant member of the fullerenes family. It is an electroactive nanomaterial with multiple redox states in a wide range of potentials undergoing six different one-electron reversible reductions to form stable intermediates [87]. Properties such as the easy functionalization and the ability for signal mediation can be exploited in the field of immunosensors [88]. An important application of functionalized  $C_{60}$  nanohybrids concerns its use as signal-amplifying tags in electrochemical immunoassays. The excellent electrochemical behavior of this material provides larger measured currents which implies a more sensitive detection, and shows electrocatalytic effects. As an example, an amino group-functionalized  $C_{60}$  prepared with 3,4,9,10-perylene-tetracarboxylic dianhydride (PTC-NH<sub>2</sub>) was used as a scaffold to immobilize the redox probe Fc-carboxylic acid and PtNPs. The resulting nanocomposite was labeled to PCT secondary antibodies in combination with GOx, showing high electrocatalytic activity towards H<sub>2</sub>O<sub>2</sub>. A sandwich configuration was constructed using an AuNPs/MWCNTs modified electrode to immobilize the capture antibody [80]. In another approach, an amino-terminated PAMAM polymer was used to prepare a  $C_{60}$  hybrid with high hydrophilicity and abundant amine groups for further modification. AuNPs were adsorbed on the hybrid and the resulting product (Au/PAMAM/ $C_{60}$ )NPs was used as a redox nanoprobe and nanocarrier to label detection antibodies (Figure 10). A sandwich-type electrochemical immunosensor for the determination of erythropoietin (EPO), an important blood doping agent, was prepared by immobilization of capture antibodies through bridging with protein A onto a GCE decorated with gold nanodendrites. The electrochemical responses were recorded after dropping tetraoctylammonium bromide (TOAB) which acted as booster to arouse the inner redox activity of Au/PAMAM/ $C_{60}$  NPs, thus providing a pair of reversible redox peaks [81].

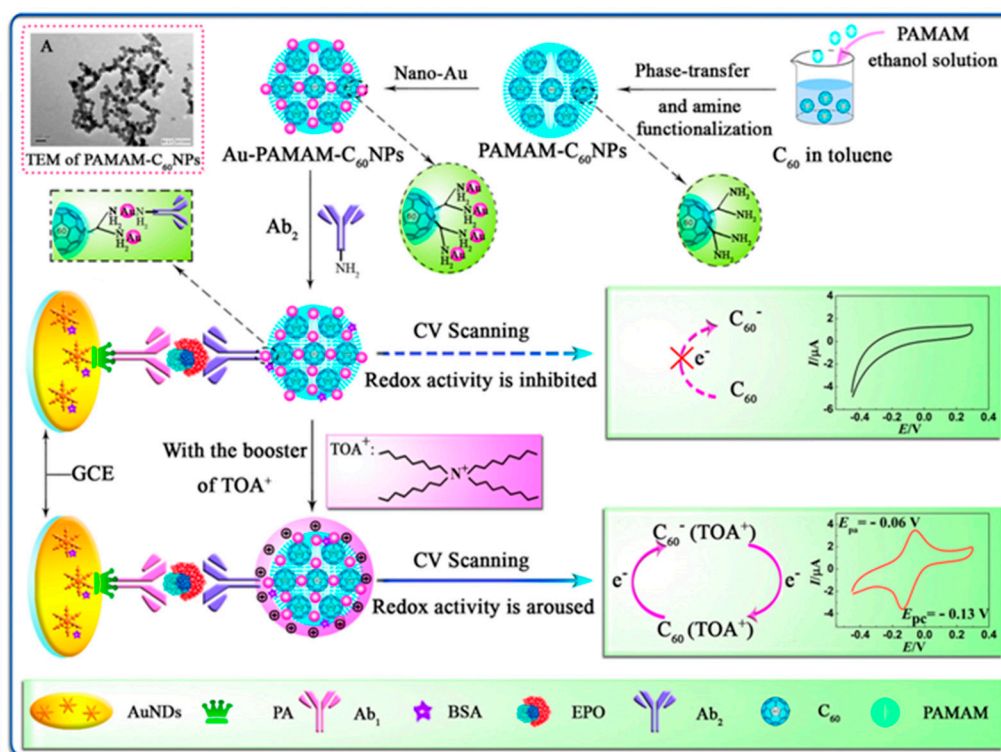


**Figure 10.** Schematic illustration of the immunosensor preparation process using bioconjugates of detector antibodies (Ab<sub>2</sub>) and (Au/PAMAM/ $C_{60}$ )NPs as advanced labels and mechanism of electrochemical reaction. See the text for more information. Reprinted from [81] with permission.

Graphene quantum dots (GQDs) are 0D materials formed by small pieces of graphene with lateral size less than 100 nm, whose properties derive from those of graphene and carbon dots (CDs) [89]. Due to quantum confinement and edge effects, this nanomaterial exhibits unique properties distinct



than those of graphene and graphene oxide. Furthermore, compared to conventional semiconductor quantum dots, QDs possess various relevant advantages for biosensing such as good biocompatibility, low toxicity, high specific surface area and easy bio-conjugation. A representative example is the preparation of a sandwich electrochemical immunosensor for the detection of avian leukosis virus subgroup J (ALVs-J). This immunosensor used QDs and apoferritin-encapsulated Cu nanoparticles for signal amplification [82]. Cu-apoferritin nanoparticles and secondary ALVs-J antibodies ( $Ab_2$ ) were immobilized onto  $Fe_3O_4@QDs$  employed as electroactive probes. After immunocomplex formation, Cu ions were released from the apoferritin cavity by immersion in an HCl solution of pH 2, and quantified by DPV. A high sensitivity (LOD of  $115\text{ TCID}_{50}\text{ mL}^{-1}$ , with  $TCID_{50}$  being the median tissue culture infective dose that produce pathological change in 50% of cell cultures inoculated) was achieved and is attributable not only to the large surface area of QDs, thus allowing a large loading of antibodies onto the  $Fe_3O_4@QDs$ , but also to the presence of Cu-apoferritin nanoparticles that significantly increased the amount of electroactive probes.

The attractiveness of carbon nanoparticles (CNPs) for the construction of electrochemical sensors comes from the confluence of interesting properties such as the electrocatalytic activity, the possibility of functionalization or doping, the ease of synthesis using environmentally friendly methods and the relatively low production costs. In the particular case of biosensors, it is also necessary to mention the ability for biomolecules immobilization and the demonstrated electron shuttle between electrode substrates and adsorbed biomolecules [90]. Although there is a wide variety of CNPs, there are still very few applications in the field of electrochemical immunosensors. The enhancement of conductivity and electron transfer promotion are the two main features to profit from when CNPs are used in the preparation of immunosensors. The combination with other materials such as metallic nanoparticles or polymers to form CNPs composites may improve their inherent properties and can enhance both the loading with biomolecules and the occurrence of the involved electrochemical reaction. The most recent applications of CNPs are devoted to designing signal amplification schemes. In this context, the main advantage relies on the possibility to immobilize a large number of biomolecules labeled with enzymes and the subsequent increase in the magnitude of electrochemical response by linking secondary antibodies in sandwich-type immunoassays. An illustrative example can be found in the development of an electrochemical immunosensor for the determination of phosphorylated p53 [83]. Carboxylated carbon nanospheres (HOOC-CNS) were obtained from fructose and used to co-link HRP and a secondary antibody ( $Ab_2$ ) for signal amplification. Primary anti-phospho-p53 antibody ( $Ab_1$ ) was covalently immobilized onto functionalized magnetic microbeads (HOOC-MBs) and the immunocomplex formation was detected upon conjugation of MBs- $Ab_1$ -phospho-p53 with HRP-CNS- $Ab_2$  by SWV after addition of  $H_2O_2$ . A similar strategy using CNS synthesized from glucose was also reported to improve the sensitivity of an electrochemical immunosensor for microcystin-LR determination.

Microcystins (MCs) are a type of toxic cyclic heptapeptides produced by cyanobacteria. Among these toxins, microcystin-LR (MC-LR) is one of the most toxic causing poisoning and even death [91]. A fast and sensitive electrochemical immunosensor for MC-LR was prepared combining the excellent electron transfer properties of GR with the good biocompatibility of CNS. Signal amplification was achieved by means of HRP-CNS- $Ab_2$  immunoconjugates. In this case, a GCE was modified with graphene sheets and chitosan and used as scaffold for the immobilization of the antigen. An indirect competitive assay was implemented with signal amplification allowing an LOD of  $0.016\text{ }\mu\text{g}\cdot\text{L}^{-1}$  to be obtained. The method was successfully applied to the detection of MC-LR in water samples [84]. Furthermore, an electrochemical immunosensor for benzo[a]pyrene (BaP) was constructed using HRP-CNS- $Ab_2$  conjugates prepared from highly carbonized nanospheres (HCS) as the signal tag. A  $Fe_3O_4$ NPs/PANI/Nafion-modified ITO electrode was also used to immobilize BaP and develop a competitive immunoassay. The enhanced current signal was achieved by means of  $Fe_3O_4$ NPs/PANI, which greatly increases the surface area of the sensing platform, as well as the large number of multi-enzyme carbon nanoparticles, and the functioning of  $Fe_3O_4$  as a biomimetic peroxidase [85].



Another strategy has been reported for an immunosensor for human IgG that consisted of preparing an AuNPs/CNS composite used as a label and a SPCE modified with polyethylene glycol (PEG) as an electrochemical platform. With a sandwich-type immunoassay, the analyte and the labeled Ab<sub>2</sub> were successively bound, and AuNPs were finally electrooxidized in 0.1 M HCl to produce Au (III) and detected by DPV with signal amplification [5].

Different fundamentals were applied to develop another immunosensor for hIgG involving Prussian blue-functionalized mesoporous carbon nanospheres (PB-MCN) coated with PDDA polyelectrolyte and AuNps. The surface negative charge of PB-MCN allowed the deposition of a positive PDDA layer which further interacts with negatively-charged colloidal gold nanoparticles obtained in citrate medium. The resulting PB-MCN/PDDA/AuNPs nanocomposite allowed the immobilization of large secondary antibodies (anti-hIgG Ab<sub>2</sub>) and glucose oxidase (GOx) loadings. A sandwich-type immunosensor using anti-IgG Ab<sub>1</sub> capture antibodies immobilized onto an AuNPs/SPCE was constructed. A DPV analytical readout was obtained after addition of glucose profiting the as peroxidase functioning of Prussian blue and the consequent Prussian blue-mediated GOx catalytic reaction. The high loadings of Prussian blue and GOx on the nanoprobe together with the enzymatically catalytic cycle greatly amplified the sensitivity of the assay, providing a detection limit of 7.8 pg·mL<sup>-1</sup> hIgG [6].

A carbon-gold nanocomposite (CGN) was prepared by a simple microwave-assisted carbonization of glucose and deposition of AuNPs for the simultaneous determination of three cancer biomarkers. The resulting CGN showed a great adsorption ability to the redox probes, thionine, DAP (2,3-diaminophenazine), and Cd<sup>2+</sup>, used respectively for the detection of CEA, PSA and AFP, whereas AuNPs decorated on the nanocomposite provided extra binding sites for immobilization of the three respective antibodies. An electrochemical platform prepared by modification of a GCE with rGO and the ionic liquid 1-aminopropyl-3-methylimidazolium chloride was used for immobilization of the capture antibodies. A sandwich-type immunoassay was performed which allowed simultaneous detection of the three antigens by SWV with LOD values at the pg·mL<sup>-1</sup> level [86].

#### 4. General Conclusions and Future Prospects

The examples compiled in this review demonstrate that carbon nanomaterials and their nanocomposites have been exploited both as mere carriers of signaling labels of different nature (HRP, ALP, HRP mimicking analogues such as hemin, ferritin and FeTMPyP and electroactive metal nanoparticles) or as tracers based on their direct electrochemistry (GONPs) for signal amplification in electrochemical DNA- and immuno-biosensing. It is worth mentioning at this point that the advantages and/or drawbacks offered by carbon nanostructures for tagging in electrochemical biosensing (discussed in deep throughout the text both in the introductory sections and in the selected examples), are closely related with many particular variables like the selected bioreceptor, assay format, and electrochemical technique used, as well as, of course, the target analyte and sample matrix. Therefore, although experience in this field could help in some way, the wide variability of approaches, applications and capacities makes it extremely difficult to choose or recommend a priori the best material and modification. Indeed, selection should be made depending on the particular application and only by experimental testing.

Apart from well-known carbon nanomaterials (CNTs and graphene) largely employed in the fabrication of electrochemical biosensors, other less common carbon nanoforms (CNHs, C<sub>60</sub>, GQDs, CNPs, MCN, CGN) have also demonstrated recently their unique features and suitability as nanolabels for enhancing sensitivity in electrochemical immunosensing approaches. Continuous efforts made in developing and understanding the properties and electrochemistry of new carbon nanomaterials and improving the reproducibility in the production and bioconjugation of monodispersed carbon nanomaterials with repeatable structure and physicochemical properties in different batches will play major roles in enhancing the analytical performance and robustness of these biosensing approaches reported so far. Other important challenges to be faced include the development of strategies

designed to minimize non-specific adsorptions of co-existing species in the complex samples on the nanomaterials due to their large surface area. Furthermore, although a large number of carbon nanomaterials have already been used for tagging in electrochemical biosensing, other nanomaterials fabricated recently like the porous ZIF-8 nanopolyhedra and the related carbon nanopolyhedra [92] will offer tremendous opportunities to be explored in this field because of their high surface area and pore volume. It will be also highly desirable to evaluate the use of carbon-nanomaterials as tags in automatic and high-throughput multi-analyte electrochemical bioanalysis and their biocompatibility also for future in vivo analysis.

However, the unique combination and integration of nanotechnology with biology and electrochemical analytical methodologies is expected to produce major advances in this field of rapid development, interest and progress and open up tremendous opportunities not only from a scientific point of view but also from a market perspective in terms of developing POC devices.

In the near future, advances in fundamental knowledge of new nanomaterials along with a focus on practical applications in real-world systems will drive electrochemical biosensing to breakthroughs in many fields of relevance. As a logical consequence of the incessant flow of impressive ideas and innovations in this burgeoning 'electrochemical biosensing industry' it looks like this field will keep on advancing for the foreseeable future. It is also expected that future innovative research in this field will couple with other major technological advances, such as integration with real-time monitoring, lateral-flow, lab-on-chip, and 3D printing techniques for the development of next-generation biosensors that are also suitable for in vivo studies.

**Acknowledgments:** The financial support of the CTQ2015-70023-R and CTQ2015-64402-C2-1-R (Spanish Ministerio de Economía y Competitividad Research Projects) and S2013/MT3029 (NANOAVANSENS Program from the Comunidad de Madrid) are gratefully acknowledged.

**Conflicts of Interest:** The authors declare no conflict of interest.

## References

1. Wu, L.; Xiong, E.H.; Zhang, X.; Zhang, X.H.; Chen, J.H. Nanomaterials as signal amplification elements in DNA-based electrochemical sensing. *NanoToday* **2014**, *9*, 197–211. [[CrossRef](#)]
2. Holzinger, H.; Le Goff, A.; Cosnier, S. Nanomaterials for biosensing applications: A review. *Front. Chem.* **2014**, *2*, 63. [[CrossRef](#)] [[PubMed](#)]
3. Adhikari, B.-R.; Govindhan, M.; Chen, A. Carbon nanomaterials based electrochemical sensors/biosensors for the sensitive detection of pharmaceutical and biological compounds. *Sensors* **2015**, *15*, 22490–22508. [[CrossRef](#)]
4. Cui, R.J.; Liu, C.; Shen, J.M.; Gao, D.; Zhu, J.J.; Chen, H.Y. Gold nanoparticle-colloidal carbon nanosphere hybrid material: preparation, characterization, and application for an amplified electrochemical immunoassay. *Adv. Funct. Mater.* **2008**, *18*, 2197–2204. [[CrossRef](#)]
5. Xu, Q.; Yan, F.; Lei, J.; Leng, C.; Ju, H. Disposable electrochemical immunosensor by using carbon sphere/gold nanoparticle composites as labels for signal amplification. *Chem. Eur. J.* **2012**, *18*, 4994–4998. [[CrossRef](#)] [[PubMed](#)]
6. Lai, G.; Zhang, H.; Yu, A.; Ju, H. In situ deposition of Prussian blue on mesoporous carbon nanosphere for sensitive electrochemical immunoassay. *Biosens. Bioelectron.* **2015**, *74*, 660–665. [[CrossRef](#)] [[PubMed](#)]
7. Wang, Y.; He, X.; Wang, K.; Ni, X.; Su, J.; Chen, Z. Ferrocene-functionalized SWCNT for electrochemical detection of T4 polynucleotide kinase activity. *Biosens. Bioelectron.* **2012**, *32*, 213–218. [[CrossRef](#)] [[PubMed](#)]
8. Lee, A.-C.; Du, D.; Chen, B.; Heng, C.-K.; Lim, T.-M.; Lin, Y. Electrochemical detection of leukemia oncogenes using enzyme-loaded carbon nanotube labels. *Analyst* **2014**, *139*, 4223–4230. [[CrossRef](#)]
9. Gao, W.; Dong, H.; Lei, J.; Ji, H.; Ju, H. Signal amplification of streptavidin-horseradish peroxidase functionalized carbon nanotubes for amperometric detection of attomolar DNA. *Chem. Commun.* **2011**, *47*, 5220–5222. [[CrossRef](#)] [[PubMed](#)]
10. Wang, Q.; Lei, J.; Deng, S.; Zhang, L.; Ju, H. Graphene-supported ferric porphyrin as a peroxidase mimic for electrochemical DNA biosensing. *Chem. Commun.* **2013**, *49*, 916–918. [[CrossRef](#)] [[PubMed](#)]

11. Zhou, Y.; Wang, M.; Xu, Z.; Ni, C.; Yin, H.; Ai, S. Investigation of the effect of phytohormone on the expression of microRNA-159a in *Arabidopsis thaliana* seedlings based on mimic enzyme catalysis systematic electrochemical biosensor. *Biosens. Bioelectron.* **2014**, *54*, 244–250. [[CrossRef](#)] [[PubMed](#)]
12. Bonanni, A.; Chua, C.K.; Zhao, G.; Sofer, Z.; Pumera, M. Inherently Electroactive Graphene Oxide Nanoplatelets as Labels for Single Nucleotide Polymorphism Detection. *ACS Nano* **2012**, *6*, 8546–8551. [[CrossRef](#)] [[PubMed](#)]
13. Loo, A.H.; Bonanni, A.; Pumera, M. Thrombin aptasensing with inherently electroactive graphene oxide nanoplatelets as labels. *Nanoscale* **2013**, *5*, 4758–4762. [[CrossRef](#)]
14. Chen, J.R.; Jiao, X.X.; Luo, H.Q.; Li, N.B. Probe-label-free electrochemical aptasensor based on methylene blue-anchored graphene oxide amplification. *J. Mater. Chem. B* **2013**, *1*, 861–864. [[CrossRef](#)]
15. Li, W.; Wu, P.; Zhang, H.; Cai, C. Signal Amplification of Graphene Oxide Combining with Restriction Endonuclease for Site-Specific Determination of DNA Methylation and Assay of Methyltransferase Activity. *Anal. Chem.* **2012**, *84*, 7583–7590. [[CrossRef](#)] [[PubMed](#)]
16. Wang, J.; Liu, G.; Jan, M.R. Ultrasensitive Electrical Biosensing of Proteins and DNA: Carbon-Nanotube Derived Amplification of the Recognition and Transduction Events. *J. Am. Chem. Soc.* **2004**, *126*, 3010–3011. [[CrossRef](#)] [[PubMed](#)]
17. Munge, B.; Liu, G.; Collins, G.; Wang, J. Multiple Enzyme Layers on Carbon Nanotubes for Electrochemical Detection Down to 80 DNA Copies. *Anal. Chem.* **2005**, *77*, 4662–4666. [[CrossRef](#)]
18. Fu, J.L.; Liu, M.H.; Liu, Y.; Woodbury, N.W.; Yan, H. Interenzyme Substrate Diffusion for an Enzyme Cascade Organized on Spatially Addressable DNA Nanostructures. *J. Am. Chem. Soc.* **2012**, *134*, 5516–5519. [[CrossRef](#)] [[PubMed](#)]
19. Yuan, Y.; Yuan, R.; Chai, Y.; Zhuo, Y.; Gan, X.; Bai, L. 3,4,9,10-Perylenetetracarboxylic Acid/Hemin Nanocomposites Act as Redox Probes and Electrocatalysts for Constructing a Pseudobioenzyme-Channeling Amplified Electrochemical Aptasensor. *Chem. Eur. J.* **2012**, *18*, 14186–14191. [[CrossRef](#)] [[PubMed](#)]
20. Travascio, P.; Li, Y.F.; Sen, D. DNA-enhanced peroxidase activity of a DNA aptamer-hemin complex. *Chem. Biol.* **1998**, *5*, 505–517. [[CrossRef](#)]
21. Pei, X.; Zhang, B.; Tang, J.; Liu, B.; Lai, W.; Tang, D. Sandwich-type immunosensors and immunoassays exploiting nanostructure labels: A review. *Anal. Chim. Acta* **2013**, *758*, 1–18. [[CrossRef](#)] [[PubMed](#)]
22. Lei, J.; Ju, H. Signal amplification using functional nanomaterials for biosensing. *Chem. Soc. Rev.* **2012**, *41*, 2122–2134. [[CrossRef](#)] [[PubMed](#)]
23. Ding, L.; Bond, A.M.; Zhai, J.; Zhang, J. Utilization of nanoparticle labels for signal amplification in ultrasensitive electrochemical affinity biosensors: A review. *Anal. Chim. Acta* **2013**, *797*, 1–12. [[CrossRef](#)] [[PubMed](#)]
24. Fenzl, C.; Hirsch, T.; Baeumner, A.J. Nanomaterials as versatile tools for signal amplification in (bio)analytical applications. *TrAC Trends Anal. Chem.* **2016**, *79*, 306–316. [[CrossRef](#)]
25. Huo, X.; Liu, X.; Liu, J.; Sukumaran, P.; Alwarappan, S.; Wong, D.K.Y. Strategic applications of nanomaterials as sensing platforms and signal amplification markers at electrochemical immunosensors. *Electroanalysis* **2016**, *28*, 1–21. [[CrossRef](#)]
26. Malhotra, R.; Patel, V.; Vaqué, J.P.; Gutkind, J.S.; Rusling, J.F. Ultrasensitive electrochemical immunosensor for oral cancer biomarker IL-6 using carbonnanotube forest electrodes and multilabel amplification. *Anal. Chem.* **2010**, *82*, 3118–3123. [[CrossRef](#)] [[PubMed](#)]
27. Kenneth, M.K.; Kenneth, M.I.; Elliott, K. Epstein-barr virus latent membrane protein 1 is essential for B-lymphocyte growth transformation. *Proc. Natl. Acad. Sci. USA* **1993**, *90*, 9150–9154.
28. Zhang, X.; Zhou, D.; Sheng, S.; Yang, J.; Chen, X.; Xie, G.; Xiang, H. Electrochemical immunoassay for the cancer marker LMP-1 (Epstein-Barr virus-derived latent membrane protein 1) using a glassy carbon electrode modified with Pd@Pt nanoparticles and a nanocomposite consisting of graphene sheets and MWCNTs. *Microchim. Acta* **2016**, *183*, 2055–2062. [[CrossRef](#)]
29. Akter, R.; Jeong, B.; Choi, J.-S.; Rahman, M.D.A. Ultrasensitive nanoimmunosensor by coupling non-covalent functionalized graphene oxide platform and numerous ferritin labels on carbon nanotubes. *Biosens. Bioelectron.* **2016**, *80*, 123–130. [[CrossRef](#)] [[PubMed](#)]
30. Feng, D.; Li, L.; Fang, X.; Han, X.; Zhang, Y. Dual signal amplification of horseradish peroxidase functionalized nanocomposite as trace label for the electrochemical detection of carcinoembryonic antigen. *Electrochim. Acta* **2014**, *127*, 334–341. [[CrossRef](#)]

31. Feng, D.; Li, L.; Zhao, J.; Zhang, Y. Simultaneous electrochemical detection of multiple biomarkers using gold nanoparticles decorated multiwall carbon nanotubes as signal enhancers. *Anal. Biochem.* **2015**, *482*, 48–54. [[CrossRef](#)] [[PubMed](#)]
32. Lai, G.; Wu, J.; Ju, H.; Yan, F. Streptavidin-functionalized silver-nanoparticle-enriched carbon nanotube tag for ultrasensitive multiplexed detection of tumor markers. *Adv. Funct. Mater.* **2011**, *21*, 2938–2943. [[CrossRef](#)]
33. Yang, P.; Li, X.; Wang, L.; Wu, Q.; Chen, Z.; Lin, X. Sandwich-type amperometric immunosensor for cancer biomarker based on signal amplification strategy of multiple enzyme-linked antibodies as probes modified with carbon nanotubes and concanavalin A. *J. Electroanal. Chem.* **2014**, *732*, 38–45. [[CrossRef](#)]
34. Li, N.; Wang, Y.; Cao, W.; Zhang, Y.; Yan, T.; Du, B.; Wei, Q. An ultrasensitive electrochemical immunosensor for CEA using MWCNT-NH<sub>2</sub> supported PdPt nanocages as labels for signal amplification. *J. Mater. Chem. B* **2015**, *3*, 2006–2011. [[CrossRef](#)]
35. Han, J.; Jiang, L.; Li, F.; Wang, P.; Liu, Q.; Dong, Y.; Li, Y.; Wei, Q. Ultrasensitive non-enzymatic immunosensor for carcino-embryonic antigen based on palladium hybrid vanadium pentoxide/multiwalled carbon nanotubes. *Biosens. Bioelectron.* **2016**, *77*, 1104–1111. [[CrossRef](#)] [[PubMed](#)]
36. Li, F.; Han, J.; Jiang, L.; Wang, Y.; Li, Y.; Dong, Y.; Wei, Q. An ultrasensitive sandwich-type electrochemical immunosensor based on signal amplification strategy of gold nanoparticles functionalized magnetic multi-walled carbon nanotubes loaded with lead ions. *Biosens. Bioelectron.* **2015**, *68*, 626–632. [[CrossRef](#)] [[PubMed](#)]
37. Jiang, L.; Han, J.; Li, F.; Gao, J.; Li, Y.; Dong, Y.; Wei, Q. A sandwich-type electrochemical immunosensor based on multiple signal amplification for  $\alpha$ -fetoprotein labeled by platinum hybrid multiwalled carbon nanotubes adhered copper oxide. *Electrochim. Acta* **2015**, *160*, 7–14. [[CrossRef](#)]
38. Tu, M.-C.; Chen, H.-Y.; Wang, Y.; Moochhala, S.M.; Alagappan, P.; Liedberg, B. Immunosensor based on carbon nanotube/manganese dioxide electrochemical tags. *Anal. Chim. Acta* **2015**, *5*, 228–233. [[CrossRef](#)] [[PubMed](#)]
39. Yang, F.; Chai, Y.; Yuan, R.; Han, J.; Yuan, Y.; Liao, N.; Yang, Z. Ultrasensitive electrochemical immunosensors for clinical immunoassay using gold nanoparticle coated multi-walled carbon nanotubes as labels and horseradish peroxidase as an enhancer. *Anal. Methods* **2013**, *5*, 5279–5285. [[CrossRef](#)]
40. Zhang, B.; He, Y.; Liu, B.; Tang, D. NiCoBP-doped carbon nanotube hybrid: A novel oxidase mimetic system for highly efficient electrochemical immunoassay. *Anal. Chim. Acta* **2014**, *851*, 49–56. [[CrossRef](#)] [[PubMed](#)]
41. Yang, H.; Yuan, R.; Chai, Y.; Su, H.; Zhuo, Y.; Jiang, W.; Song, Z. Electrochemical immunosensor for human chorionic gonadotropin based on horseradish peroxidase-functionalized Prussian blue-carbon nanotubes/gold nanocomposites as labels for signal amplification. *Electrochim. Acta* **2011**, *56*, 1973–1980. [[CrossRef](#)]
42. Zhu, Y.; Son, J.I.; Shim, Y.B. Amplification strategy based on gold nanoparticle-decorated carbon nanotubes for neomycin immunosensors. *Biosens. Bioelectron.* **2010**, *26*, 1002–1008. [[CrossRef](#)] [[PubMed](#)]
43. Zhang, X.; Shen, J.; Ma, H.; Jiang, Y.; Huang, C.; Han, E.; Yao, B.; He, Y. Optimized dendrimer-encapsulated gold nanoparticles and enhanced carbon nanotube nanoprobe for amplified electrochemical immunoassay of *E. coli* in dairy product based on enzymatically induced deposition of polyaniline. *Biosens. Bioelectron.* **2016**, *80*, 666–673. [[CrossRef](#)] [[PubMed](#)]
44. Leng, C.; Wu, J.; Xu, Q.; Lai, G.; Ju, H.; Yan, F. A highly sensitive disposable immunosensor through direct electro-reduction of oxygen catalyzed by palladium nanoparticle decorated carbon nanotube label. *Biosens. Bioelectron.* **2011**, *27*, 71–76. [[CrossRef](#)] [[PubMed](#)]
45. Ball, D.; Rose, E.; Alpert, E.  $\alpha$ -Fetoprotein levels in normal adults. *Am. J. Med. Sci.* **1992**, *303*, 157–159. [[CrossRef](#)] [[PubMed](#)]
46. Karyakin, A.A.; Gitelmacher, O.V.; Karyakina, E.E. Prussian blue based first-generation biosensor—A sensitive amperometric electrode for glucose. *Anal. Chem.* **1995**, *67*, 2419–2423. [[CrossRef](#)]
47. Wei, T.; Dai, Z.; Lin, Y.; Du, D. Electrochemical immunoassays based on graphene: A review. *Electroanalysis* **2016**, *28*, 4–12. [[CrossRef](#)]
48. Liu, Y.; Man, H.; Gao, J.; Wu, D.; Ren, X.; Yan, T.; Pang, X.; Wei, Q. Ultrasensitive electrochemical immunosensor for SCCA detection based on ternary Pt/PdCu nanocube anchored on three-dimensional graphene framework for signal amplification. *Biosens. Bioelectron.* **2016**, *79*, 71–78. [[CrossRef](#)] [[PubMed](#)]

49. Duk, J.M.; Aalders, J.G.; Fleuren, G.J.; Krans, M.; DEBruijn, H.W. Tumor markers CA 125, squamous cell carcinoma antigen, and carcinoembryonic antigen in patients with adenocarcinoma of the uterine cervix. *Obstet. Gynecol.* **1989**, *73*, 661–668. [[PubMed](#)]
50. Lai, G.; Cheng, H.; Xin, D.; Zhang, H.; Yu, A. Amplified inhibition of the electrochemical signal of ferrocene by enzyme-functionalized graphene oxide nanoprobe for ultrasensitive immunoassay. *Anal. Chim. Acta* **2016**, *902*, 189–195. [[CrossRef](#)] [[PubMed](#)]
51. Buccheri, G.; Ferrigno, D. Monitoring lung cancer with tissue polypeptide anti-gen: An ancillary, profitable serum test to evaluate treatment response and posttreatment disease status. *Lung Cancer* **1995**, *13*, 155–168. [[CrossRef](#)]
52. Sawant, S.S.; Chaukar, D.A.; Joshi, S.S.; Dange, P.P.; Kannan, S.; Kane, S.; D'Cruz, A.K.; Vaidya, M.M. Pro-gnostic value of tissue polypeptide antigen in oral squamous cell carcinoma. *Oral Oncol.* **2011**, *47*, 114–120. [[CrossRef](#)] [[PubMed](#)]
53. Wang, Y.; Wang, Y.; Pang, X.; Du, B.; Li, H.; Wu, D.; Wei, Q. Ultrasensitive sandwich-type electrochemical immunosensor based on dual signal amplification strategy using multifunctional graphene nanocomposites as labels for quantitative detection of tissue polypeptide. *Sens. Actuators B Chem.* **2015**, *214*, 124–131. [[CrossRef](#)]
54. Jiricny, J. An APE that proofreads. *Nature* **2002**, *415*, 593–594. [[CrossRef](#)] [[PubMed](#)]
55. Zhong, Z.; Li, M.; Qing, Y.; Dai, N.; Guan, W.; Liang, W.; Wang, D. Signal-on electrochemical immunoassay for APE1 using ionic liquid doped Au nanoparticle/graphene as a nanocarrier and alkaline phosphatase as enhancer. *Analyst* **2014**, *139*, 6563–6568. [[CrossRef](#)] [[PubMed](#)]
56. Li, L.; Zhang, L.; Yu, J.; Ge, S.; Song, X. All-graphene composite materials for signal amplification toward ultrasensitive electrochemical immunosensing of tumor marker. *Biosens. Bioelectron.* **2015**, *71*, 108–114. [[CrossRef](#)] [[PubMed](#)]
57. Gao, Q.; Liu, N.; Ma, Z. Prussian blue–gold nanoparticles-ionic liquid functionalized reduced graphene oxide nanocomposite as label for ultrasensitive electrochemical immunoassay of  $\alpha$ -fetoprotein. *Anal. Chim. Acta* **2014**, *829*, 15–21. [[CrossRef](#)] [[PubMed](#)]
58. Shen, G.; Hu, X.; Zhang, S. A signal-enhanced electrochemical immunosensor based on dendrimer functionalized-graphene as a label for the detection of  $\alpha$ -1-fetoprotein. *J. Electroanal. Chem.* **2014**, *717*–*718*, 172–176. [[CrossRef](#)]
59. Li, M.; Wang, P.; Li, F.; Chu, Q.; Li, Y.; Dong, Y. An ultrasensitive sandwich-type electrochemical immunosensor based on the signal amplification strategy of mesoporous core-shell Pd@Pt nanoparticles/amino group functionalized graphene nanocomposite. *Biosens. Bioelectron.* **2017**, *87*, 752–759. [[CrossRef](#)] [[PubMed](#)]
60. Chen, X.; Jia, X.; Han, J.; Ma, J.; Man, Z. Electrochemical immunosensor for simultaneous detection of multiplex cancer biomarkers based on graphene nano composites. *Biosens. Bioelectron.* **2013**, *50*, 356–361. [[CrossRef](#)] [[PubMed](#)]
61. Jia, X.; Chen, X.; Han, J.; Ma, J.; Man, Z. Triple signal amplification using gold nanoparticles, bienzyme and platinum nanoparticles functionalized graphene as enhancers for simultaneous multiple electrochemical immunoassay. *Biosens. Bioelectron.* **2014**, *53*, 65–70. [[CrossRef](#)] [[PubMed](#)]
62. Sun, G.; Zhang, L.; Zhang, Y.; Yang, H.; Ma, C.; Ge, S.; Yan, M.; Yu, J.; Song, X. Multiplexed enzyme-free electrochemical immunosensor based on ZnO nanorods modified reduced graphene oxide-paper electrode and silver deposition-induced signal amplification strategy. *Biosens. Bioelectron.* **2015**, *71*, 30–36. [[CrossRef](#)] [[PubMed](#)]
63. Zhu, Q.; Chai, Y.; Yuan, R.; Zhuo, Y.; Han, J.; Li, Y.; Liao, N. Amperometric immunosensor for simultaneous detection of three analytes in one interface using dual functionalized graphene sheets integrated with redox-probes as tracer matrixes. *Biosens. Bioelectron.* **2013**, *43*, 440–445. [[CrossRef](#)] [[PubMed](#)]
64. Yuan, G.; Yu, C.; Xia, C.; Gao, L.; Xu, W.; Li, W.; He, J. A simultaneous electrochemical multianalyte immunoassay of high sensitivity C-reactive protein and soluble CD40 ligand based on reduced graphene oxide-tetraethylene pentamine that directly adsorb metal ions as labels. *Biosens. Bioelectron.* **2015**, *72*, 237–246. [[CrossRef](#)] [[PubMed](#)]
65. Yang, Z.-H.; Zhuo, Y.; Yuan, R.; Chai, Y.-Q. An amplified electrochemical immunosensor based on in situ-produced 1-naphthol as electroactive substance and graphene oxide and Pt nanoparticles functionalized CeO<sub>2</sub> nanocomposites as signal enhancer. *Biosens. Bioelectron.* **2015**, *69*, 321–327. [[CrossRef](#)] [[PubMed](#)]



66. Huang, J.; Lin, Q.; Zhang, X.; He, X.; Xing, X.; Lian, W.; Zuo, M.; Zhang, Q. Electrochemical immunosensor based on polyaniline/poly (acrylic acid) and Au-hybrid graphene nanocomposite for sensitivity enhanced detection of salbutamol. *Food Res. Int.* **2011**, *44*, 92–97. [[CrossRef](#)]
67. Li, J.; Liu, S.; Yu, J.; Lian, W.; Cui, M.; Xu, W.; Huang, J. Electrochemical immunosensor based on graphene–polyaniline composites and carboxylated graphene oxide for estradiol detection. *Sens. Actuators B Chem.* **2013**, *188*, 99–105. [[CrossRef](#)]
68. Fang, Y.-S.; Chen, S.-Y.; Huang, X.-J.; Wang, L.-S.; Wang, H.-Y.; Wang, J.-F. Simple approach for ultrasensitive electrochemical immunoassay of *Clostridium difficile* toxin B detection. *Biosens. Bioelectron.* **2014**, *53*, 238–244. [[CrossRef](#)] [[PubMed](#)]
69. Pedrero, M.; Campuzano, S.; Pingarrón, J.M. Electrochemical biosensors for the determination of cardiovascular markers: A review. *Electroanalysis* **2014**, *26*, 1132–1153. [[CrossRef](#)]
70. Ouyang, J.; Duan, J.L.; Baeyens, W.R.G.; Delanghe, J.R. A simple method for the study of salbutamol pharmacokinetics by ion chromatography with direct conductivity detection. *Talanta* **2005**, *65*, 1–6. [[CrossRef](#)] [[PubMed](#)]
71. Iijima, S.; Yudasaka, M.; Yamada, R.; Bandow, S.; Suenaga, K.; Kokai, F.; Takahashi, K. Nano-aggregates of single-walled graphitic carbon nanohorns. *Chem. Phys. Lett.* **1999**, *309*, 165–170. [[CrossRef](#)]
72. Miyawaki, J.; Yudasaka, M.; Azami, T.; Kubo, Y.; Iijima, S. Toxicity of Single-Walled Carbon Nanohorns. *ACS Nano* **2008**, *2*, 213–226. [[CrossRef](#)] [[PubMed](#)]
73. Zhu, S.; Xu, G. Single-walled carbon nanohorns and their applications. *Nanoscale* **2010**, *2*, 2538–2549. [[CrossRef](#)] [[PubMed](#)]
74. Yáñez-Sedeño, P.; González-Cortés, A.L.; Agüí, J.M. Pingarrón, Uncommon carbon nanostructures for the preparation of electrochemical immunosensors. *Electroanalysis* **2016**, *28*, 1679–1691. [[CrossRef](#)]
75. Yang, F.; Han, J.; Zhuo, Y.; Yang, Z.; Chain, Y.; Yuan, R. Highly sensitive impedimetric immunosensor based on single-walled carbon nanohorns as labels and bienzyme biocatalyzed precipitation as enhancer for cancer biomarker detection. *Biosens. Bioelectron.* **2014**, *55*, 360–365. [[CrossRef](#)] [[PubMed](#)]
76. Zhao, C.; Lin, D.; Wu, J.; Ding, L.; Ju, H.; Yan, F. Nanogold-enriched carbon nanohorn label for sensitive electrochemical detection of biomarker on a disposable immunosensor. *Electroanalysis* **2013**, *25*, 1044–1049. [[CrossRef](#)]
77. Zhao, C.; Wu, J.; Ju, H.; Yan, F. Multiplexed electrochemical immunoassay using streptavidin/nanogold/carbon nanohorn as a signal tag to induce silver deposition. *Anal. Chim. Acta* **2014**, *847*, 37–43. [[CrossRef](#)] [[PubMed](#)]
78. Liu, F.; Xiang, G.; Yuan, R.; Chen, X.; Luo, F.; Jiang, D.; Huang, S.; Li, Y.; Pu, X. Procalcitonin sensitive detection based on graphene–gold nanocomposite film sensor platform and single-walled carbon nanohorns/hollow Pt chains complex as signal tags. *Biosens. Bioelectron.* **2014**, *60*, 210–217. [[CrossRef](#)] [[PubMed](#)]
79. Liu, F.; Xiang, G.; Chen, X.; Luo, F.; Jiang, D.; Huang, S.; Li, Y.; Pu, X. A novel strategy of procalcitonin detection based on multi-nanomaterials of single-walled carbon nanohorns-hollow Pt nanospheres/PAMAM as signal tags. *RSC Adv.* **2014**, *4*, 13934–13940. [[CrossRef](#)]
80. Li, P.; Zhang, W.; Zhou, X.; Zhang, L. C60 carboxyfullerene-based functionalised nanohybrids as signal-amplifying tags for the ultrasensitive electrochemical detection of procalcitonin. *Clin. Biochem.* **2015**, *48*, 156–161. [[CrossRef](#)] [[PubMed](#)]
81. Han, J.; Zhuo, Y.; Chai, Y.-Q.; Xiang, Y.; Yuan, R. New type of redox nanoprobe: C60-based nanomaterial and its application in electrochemical immunoassay for doping detection. *Anal. Chem.* **2015**, *87*, 1669–1675. [[CrossRef](#)] [[PubMed](#)]
82. Wang, X.; Chen, L.; Su, X.; Ai, S. Electrochemical immunosensor with graphene quantum dots and apoferritin-encapsulated Cu nanoparticles double-assisted signal amplification for detection of avian leukosis virus subgroup. *J. Biosens. Bioelectron.* **2013**, *47*, 171–177. [[CrossRef](#)] [[PubMed](#)]
83. Luo, Y.; Asiri, A.M.; Zhang, X.; Yang, G.; Du, D.; Lin, Y. A magnetic electrochemical immunosensor for the detection of phosphorylated p53 based on enzyme functionalized carbon nanospheres with signal amplification. *RSC Adv.* **2014**, *4*, 54066–54071. [[CrossRef](#)]
84. Zhao, H.; Tian, J.; Quan, X. A graphene and multienzyme functionalized carbon nanosphere-based electrochemical immunosensor for microcystin-LR detection. *Colloids Surf. B Biointerf.* **2013**, *103*, 38–44. [[CrossRef](#)] [[PubMed](#)]

85. Lin, M.; Liu, Y.; Sun, Z.; Zhang, S.; Yang, Z.; Ni, C. Electrochemical immunoassay of benzo[a]pyrene based on dual amplification strategy of electron-accelerated Fe<sub>3</sub>O<sub>4</sub>/polyaniline platform and multi-enzyme-functionalized carbon sphere label. *Anal. Chim. Acta* **2012**, *722*, 100–106. [[CrossRef](#)] [[PubMed](#)]
86. Xu, T.; Liu, N.; Yuan, J.; Man, Z. Triple tumor markers assay based on carbon-gold nanocomposite. *Biosens. Bioelectron.* **2015**, *70*, 161–166. [[CrossRef](#)] [[PubMed](#)]
87. Pilehvar, S.; De Wael, K. Recent advances in electrochemical biosensors based on fullerene-C<sub>60</sub> nano-structured platforms. *Biosensors* **2015**, *5*, 712–735. [[CrossRef](#)] [[PubMed](#)]
88. Afreen, S.; Muthoosamy, K.; Manickam, S.; Hashim, U. Functionalized fullerene (C<sub>60</sub>) as a potential nanomediator in the fabrication of highly sensitive biosensors. *Biosens. Bioelectron.* **2015**, *63*, 354–364. [[CrossRef](#)] [[PubMed](#)]
89. Sun, H.; Wu, L.; Wei, W.; Qu, X. Recent advances in graphene quantum dots for sensing. *Mater. Today* **2013**, *16*, 433–442. [[CrossRef](#)]
90. Szot, K.; Opallo, M. (Bio)electroanalytical applications of carbon nanoparticles. *Electroanalysis* **2016**, *28*, 46–57. [[CrossRef](#)]
91. Gupta, N.; Pant, S.C.; Vijayaraghavan, R.; Rao, P.V.L. Comparative toxicity evaluation of cyanobacterial cyclic peptide toxin microcystin variants (LR, RR, YR) in mice. *Toxicology* **2003**, *188*, 285–296. [[CrossRef](#)]
92. Gai, P.B.; Zhang, H.J.; Zhang, Y.S.; Liu, W.; Zhu, G.B.; Zhang, X.H.; Chen, J.H. Simultaneous electrochemical detection of ascorbic acid, dopamine and uric acid based on nitrogen doped porous carbon nanopolyhedra. *J. Mater. Chem. B* **2013**, *1*, 2742–2749. [[CrossRef](#)]



© 2017 by the authors; licensee MDPI, Basel, Switzerland. This article is an open access article distributed under the terms and conditions of the Creative Commons Attribution (CC-BY) license (<http://creativecommons.org/licenses/by/4.0/>).